



## METHOD ARTICLE

# Development of a cell-free split-luciferase biochemical assay as a tool for screening for inhibitors of challenging protein-protein interaction targets [version 1; peer review: 2 approved with reservations]

Rachel Cooley <sup>1\*</sup>, Neesha Kara <sup>1\*</sup>, Ning Sze Hui <sup>1</sup>, Jonathan Tart <sup>2</sup>,  
Chloë Roustan <sup>1</sup>, Roger George <sup>1</sup>, David C. Hancock <sup>1</sup>, Brock F. Binkowski <sup>3</sup>,  
Keith V. Wood <sup>3</sup>, Mohamed Ismail <sup>1</sup>, Julian Downward <sup>1,4</sup>

<sup>1</sup>Francis Crick Institute, London, UK

<sup>2</sup>AstraZeneca, Cambridge, UK

<sup>3</sup>Promega, Madison, Wisconsin, USA

<sup>4</sup>Institute of Cancer Research, UK, London, UK

\* Equal contributors

**v1** First published: 06 Feb 2020, 5:20  
<https://doi.org/10.12688/wellcomeopenres.15675.1>

Latest published: 02 Jun 2020, 5:20  
<https://doi.org/10.12688/wellcomeopenres.15675.2>

## Abstract

Targeting the interaction of proteins with weak binding affinities or low solubility represents a particular challenge for drug screening. The NanoLuc<sup>®</sup> Binary Technology (NanoBiT<sup>®</sup>) was originally developed to detect protein-protein interactions in live mammalian cells. Here we report the successful translation of the NanoBit cellular assay into a biochemical, cell-free format using mammalian cell lysates. We show that the assay is suitable for the detection of both strong and weak protein interactions such as those involving the binding of RAS oncoproteins to either RAF or phosphoinositide 3-kinase (PI3K) effectors respectively, and that it is also effective for the study of poorly soluble protein domains such as the RAS binding domain of PI3K. Furthermore, the RAS interaction assay is sensitive and responds to both strong and weak RAS inhibitors. Our data show that the assay is robust, reproducible, cost-effective, and can be adapted for small and large-scale screening approaches. The NanoBit Biochemical Assay offers an attractive tool for drug screening against challenging protein-protein interaction targets, including the interaction of RAS with PI3K.

## Keywords

KRAS, PI3K, RAF, protein-protein interaction, luciferase, screening

## Open Peer Review

Reviewer Status

	Invited Reviewers	
	1	2
<b>version 2</b> (revision) 02 Jun 2020	 report	 report
<b>version 1</b> 06 Feb 2020	 report	 report

- Andrew G. Stephen** , Frederick National Laboratory for Cancer Research, Frederick, USA
- Nicolas Bery** , Université Toulouse III Paul Sabatier, CNRS, Toulouse, France

Any reports and responses or comments on the article can be found at the end of the article.



This article is included in the [The Francis Crick Institute](#) gateway.

**Corresponding authors:** Mohamed Ismail ([mohamed.ismail@crick.ac.uk](mailto:mohamed.ismail@crick.ac.uk)), Julian Downward ([julian.downward@crick.ac.uk](mailto:julian.downward@crick.ac.uk))

**Author roles:** **Cooley R:** Investigation, Methodology, Writing – Review & Editing; **Kara N:** Investigation, Methodology, Writing – Review & Editing; **Hui NS:** Investigation, Methodology, Writing – Review & Editing; **Tart J:** Investigation, Methodology, Writing – Review & Editing; **Roustan C:** Investigation, Methodology, Writing – Review & Editing; **George R:** Investigation, Methodology, Writing – Review & Editing; **Hancock DC:** Investigation, Methodology, Writing – Review & Editing; **Binkowski BF:** Resources, Writing – Review & Editing; **Wood KV:** Resources, Writing – Review & Editing; **Ismail M:** Conceptualization, Data Curation, Investigation, Methodology, Project Administration, Writing – Original Draft Preparation, Writing – Review & Editing; **Downward J:** Conceptualization, Funding Acquisition, Methodology, Project Administration, Resources, Supervision, Writing – Review & Editing

**Competing interests:** Competing interests: B.F.B and K.V.W. are employees of Promega Corporation and J.T. is an employee of AstraZeneca. J.D. has acted as a consultant for AstraZeneca, Bayer, Novartis, Vividion and TheRas. None of the other authors of this manuscript have a financial interest related to this work.

**Grant information:** This work was supported by funding to JD from the Francis Crick Institute, which receives its core funding from Cancer Research UK (FC001070), the UK Medical Research Council (FC001070) and the Wellcome Trust (FC001070), from the European Research Council Advanced Grant RASIMMUNE and from a Wellcome Trust Senior Investigator Award (103799).

*The funders had no role in study design, data collection and analysis, decision to publish, or preparation of the manuscript.*

**Copyright:** © 2020 Cooley R *et al.* This is an open access article distributed under the terms of the [Creative Commons Attribution License](#), which permits unrestricted use, distribution, and reproduction in any medium, provided the original work is properly cited.

**How to cite this article:** Cooley R, Kara N, Hui NS *et al.* **Development of a cell-free split-luciferase biochemical assay as a tool for screening for inhibitors of challenging protein-protein interaction targets [version 1; peer review: 2 approved with reservations]** Wellcome Open Research 2020, 5:20 <https://doi.org/10.12688/wellcomeopenres.15675.1>

**First published:** 06 Feb 2020, 5:20 <https://doi.org/10.12688/wellcomeopenres.15675.1>

## Introduction

While enzymatic activities have generally been the preferred starting point for the development of drugs targeting biological processes, there are not always suitable tractable enzymatic targets in signalling pathways of interest. In such cases, the transfer of biological signals is likely to be also dependent on specific protein-protein interactions (PPIs), which can make attractive alternative targets for drug discovery. The selection of a suitable binding assay is a key factor in the development of screens to identify inhibitors of protein-protein interactions. The selection process for a cell-free, or biochemical, assay will depend mainly on the nature of the protein complex under investigation, in particular the binding affinities and solubilities of the components. Protein complexes with low binding affinity pose a particular challenge for drug screening assays for a number of reasons. First, for optimal biochemical assay screening, one of the protein concentrations should be close to the  $K_d$  (dissociation constant) of the complex binding affinity. At this concentration, the protein will exist in a 50% unbound and 50% complexed state, which, in the screening process, allows for detection of weakly binding compounds that disrupt the protein interaction of interest. Protein complexes with weak binding affinities (low micromolar and above) thus require large amounts of proteins for drug screening, which is not always feasible, especially for poorly soluble proteins. Second, weak binding protein complexes require more screening reagents when using biochemical assays such as HTRF (Homogeneous Time Resolved Fluorescence) which may be prohibitively expensive for high throughput screening<sup>1,2</sup>.

The RAS family of oncoproteins (HRAS, NRAS and KRAS) are key regulators of cellular proliferation and when mutationally activated, as in many cancers, can drive tumor formation. They cycle between inactive (RAS-GDP bound) and active (RAS-GTP bound) forms, with the latter contributing to a wide range of cellular signaling through direct interaction with effector enzymes such as RAF protein kinase isoforms (ARAF, BRAF and CRAF/RAF1) and members of the PI3K family of lipid kinases (p110 $\alpha$ ,  $\delta$  and  $\gamma$ ) through their RAS binding domains (RBDs), resulting in the activation of the MAPK and PI3K signaling pathways<sup>3-7</sup>. Oncogenic mutations in RAS lock it into the GTP-bound form, causing the constant activation of downstream pathways thereby contributing to the genesis of several commonly occurring types of cancer<sup>6,8,9</sup>. Therefore, finding inhibitors that can block the RAS/RAF and/or the RAS/PI3K interaction would be a significant development toward future cancer therapies<sup>10-12</sup>. However, a significant stumbling block in the quest to inhibit these protein complexes is the fact that RAS interacts with RAF and PI3K with two widely differing affinities ( $K_d \sim 20$  nM and 3  $\mu$ M respectively)<sup>13-15</sup>. The relatively weak interaction between RAS and PI3K makes this a challenging protein complex for the selection of a suitable biochemical assay for drug screening for the reason addressed above.

The Nano<sup>®</sup> assay provides a tool for detecting protein-protein interactions in live cells (Figure 1A). The assay is based on splitting the engineered luminescent protein NanoLuc<sup>®</sup> into two separate subunits, the small BiT (SmBiT, 1.3 kDa in size) and the Large BiT (LgBiT, 18 kDa in size). These SmBiT and LgBiT

subunits (hereafter Sm and Lg) interact very weakly with an affinity of  $K_d = 190$   $\mu$ M, so their assembly to form an active luminescent complex only occurs upon the interaction of the separate binding partner proteins to which they are fused. The NanoBit cellular assay has proved successful in several cellular PPI studies<sup>16</sup>. Nevertheless, cellular assays are usually more demanding, do not work for compounds that are not cell membrane permeable and do not produce the high throughput and consistency offered by biochemical assays<sup>17,18</sup>. Here we present the successful translation of the NanoBiT cellular assay to a biochemical assay, which we have termed the NanoBit Biochemical Assay (NBBA). The NBBA proves efficient in detecting both the strong and weak interactions between RAS/RAF and RAS/PI3K respectively. Furthermore, the NBBA is responsive to various types of RAS inhibitors and can be used in small and large scale screening.

## Results

Raw values for each experiment are available as *Underlying data*<sup>19</sup>.

### HTRF assay is suitable for detecting the RAS/RAF interaction but not RAS/PI3K

We chose homogeneous time-resolved fluorescence (HTRF) as an initial biochemical screening assay since it has previously been shown to be a suitable format for the measurement of active KRAS/CRAF-RBD binding interactions<sup>20</sup>. An activated form of KRAS bearing the mutation G12C and the CRAF-RBD were expressed and purified from *Escherichia coli* and the KRAS loaded with GppNHP (a non-hydrolysable GTP analogue). With KRAS at 5nM and CRAF-RBD at 10 nM we obtained a clear signal of interaction between active KRAS-G12C-GppNHP and CRAF-RBD as compared to the inactive KRAS-G12C-GDP (Figure 2A)<sup>19</sup>.

To determine if a similar specific response could be seen with p110 $\alpha$  we used the full-length p110 $\alpha$  fused to GST produced in baculovirus, as the isolated PI3K and their RBDs are known to be poorly soluble<sup>21</sup>. Since p110 $\alpha$  is not as soluble as KRAS, we kept the concentration of p110 $\alpha$  low (10 nM) and added the KRAS at 3  $\mu$ M (approximately the interaction  $K_d$ ). This posed a challenge for HTRF as the labelling reagents also needed to be at a high concentration, using large amounts of reagent and resulting in high background signals. KRAS was labelled with either streptavidin-europium or streptavidin-XL665; coupled with either p110 $\alpha$  labelled with Anti-GST XL665 or streptavidin-europium, respectively. Only a low signal was achieved (Figure 2B, C)<sup>19</sup> with KRAS-GppNHP compared to KRAS-GDP, suggesting that this approach was not promising for further follow up. Together, these results show that whilst the HTRF assay is appropriate for strong PPI, such as RAS/RAF binding, it is unsuitable for much weaker interactions such as RAS/p110 $\alpha$ .

### Translation of the NanoBiT cellular assay to a biochemical assay

To pursue the development of an assay for relatively weak protein interactions, we conducted several experiments aimed at transforming the NanoBit cellular assay into a biochemical

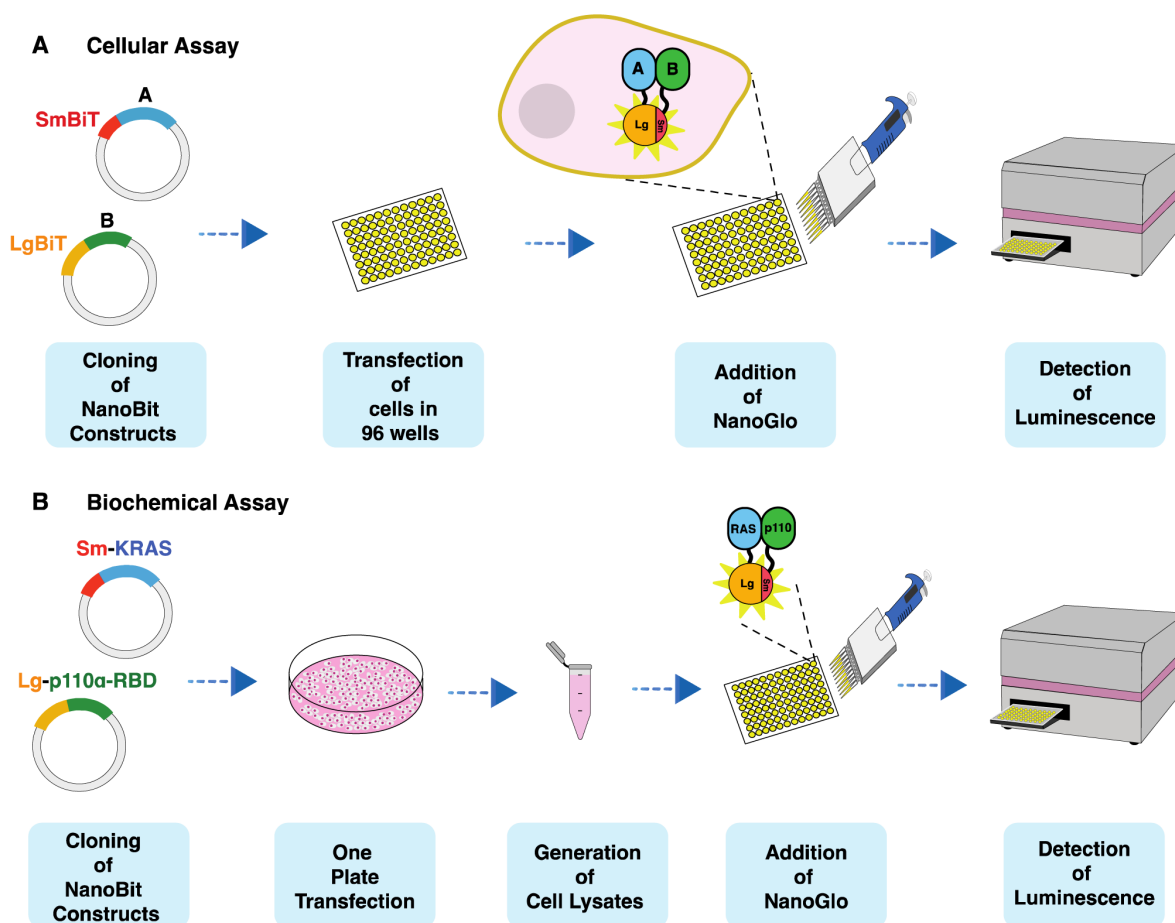


**Figure 1. Schematic diagram of the steps involved in the NanoBiT biochemical assay (NBBA).** The NanoBiT live cell assay, proteins of interest (**A** and **B**) are cloned in the NanoBiT vectors expressing either the Sm (Small-BiT) or the Lg (Large-BiT). The constructs are transfected in individual 96 well plate, followed by the addition of 25  $\mu$ l 1X Nano-Glo substrate for detecting the PPI (**A**). In contrast, in the NBBA (**B**), only one transfection is required, followed by cell lysis, quantification and titration of cell lysate into 384 well plates followed by the addition of 2 or 4  $\mu$ l of 1X Nano-Glo for 10- or 20- $\mu$ l reaction volume respectively for detecting the PPI.

assay using cell lysate from mammalian HEK293 cells. In principle, the assay involves transfecting cells with SmBiT and LgBiT expression constructs containing the target proteins of interest, followed by harvest, lysis, lysate quantification, aliquoting and addition of the Nano-Glo<sup>®</sup> Live Cell Substrate (hereafter Nano-Glo) for detection (Figure 1B). The pros and cons of using cell lysates versus live cells in PPI screens are outlined in Table 1.

We first tested the interaction of the KRAS-G12C (hereafter KRAS) oncogenic mutant with CRAF protein (hereafter RAF), to determine if the NanoBiT assay was suitable for biochemical analysis. Both KRAS and RAF were cloned into the NanoBiT vectors (BiBiT vectors system) with the orientations Lg-KRAS and Sm-RAF, respectively, and co-transfected into HEK293 cells. The Lg and the Sm tags were positioned

at the N-terminal KRAS and RAF, as RAS localizes on the cellular membrane via its C-terminal region and to ensure appropriate activation of RAF C-terminal kinase domain. Due to the strong interaction of RAS with RAF, we prepared a serial dilution of the cell lysate from 0.002–5  $\mu$ g/ $\mu$ l in 20  $\mu$ l reaction volumes<sup>13</sup>.

In addition, we used only 4  $\mu$ l of 1X Nano-Glo rather than the 25  $\mu$ l that is required for live cells. We detected a clear signal increase of the Lg-KRAS/Sm-RAF interaction starting from 156 ng/ $\mu$ l cell lysate concentration and a lack of signal from the Sm/Lg BiT alone (Figure 3A)<sup>19</sup>. We then proceeded to perform a time course of the Lg-KRAS/Sm-RAF cell lysate to determine the half-life of the Nano-Glo signal. We found the signal to increase during the first 5 min of reaction and to fall again after 20 min (Figure 3B)<sup>19</sup>.

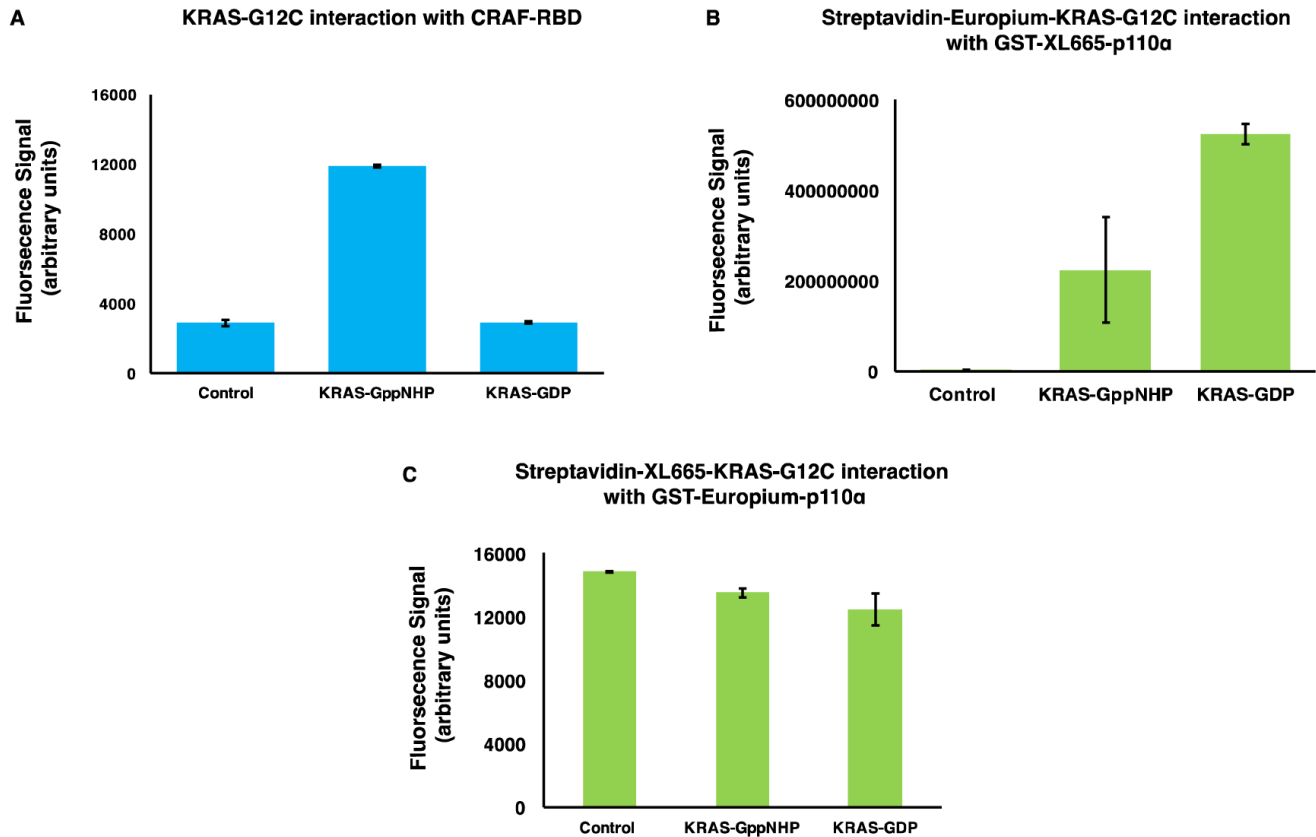


**Figure 2. The homogenous time-resolved fluorescence (HTRF) assay is suitable for detecting the interaction of KRAS/CRAF but not KRAS/p110 $\alpha$ .** All data are produced from replicates (n=4). **(A)** 5 nM Avi-KRAS was loaded with either GppNHP (GTP analogue) or GDP was labelled with streptavidin-Europium (donor beads), and mixed with 10 nM labelled GST-CRAF-RBD with anti-GST XL665 (acceptor beads). Control, contains are the donor and acceptor beads with TB (titration buffer). There is a clear signal of CRAF-RBD with KRAS\_GppNHP but not with KRAS\_GDP. **(B)** 3  $\mu$ M Streptavidin-Europium-KRAS\_GppNHP or KRAS\_GDP with 10 nM anti-GST XL665-p110 $\alpha$ . The signal of fluorescence was too high due to the high concentration of Europium used in the experiments. **(C)** 10 nM GST-Europium-p110 $\alpha$  mixed with Streptavidin-XL665- KRAS\_GppNHP or KRAS\_GDP. The signal is lower than the experiment in **(C)**; however, the difference between the control (TB buffer or KRAS-GDP) and the positive interaction is very narrow, which makes it unsuitable for drug screening.

**Table 1. The advantages and disadvantages of the NanoBIT cellular assay vs the NanoBIT biochemical assay.**

Live cell monolayer	Cell lysate (biochemical)
Working with monolayer cells is costly – in particular transfection reagents, Nano-Glo reagent and cell culture plates.	Relatively cost effective as large amounts of transfection reagent and Nano-Glo reagent are not required.
Technically challenging for high throughput screening – needs to be compatible with work under a sterile environment.	Suitable for high throughput screening and does not necessitate extensive work under sterile environment.
Time consuming – takes up to two days to seed and transfect cells.	Time efficient - lysate can be generated in bulk, aliquoted and stored in -80 for multiple usages.
Transfection efficiency may vary among wells, giving inconsistent results.	Transfection is only performed once, so all wells contain a uniform lysate.
Limited control over protein expression levels.	Protein concentration can be optimized by diluting the cell lysate in lysis buffer.
Proteins will be expressed in their natural environment, and	will have undergone all post translational modifications.
Positive hits obtained from the monolayer cells will indicate that they are also cell penetrable.	The positive hits from the cell lysate will give no indication if they are cell penetrable

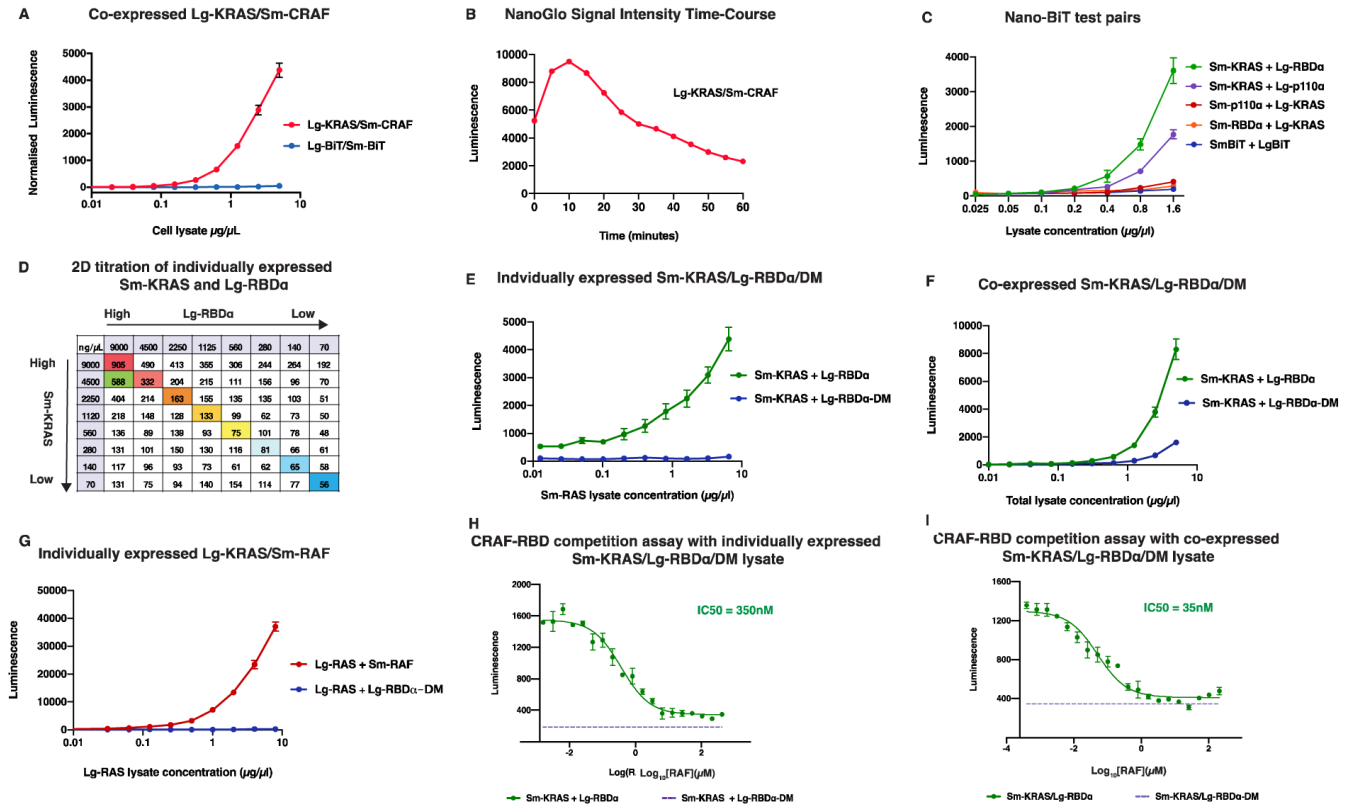


**Figure 3. NanoBit biochemical assay (NBBA) expression, protein-protein interaction (PPI) detection and competition assay.** (A) Titration of HEK293 cell lysate co-expressing Lg-KRAS/Sm-CRAF (1–5000 ng/ $\mu$ l). The negative control is the lysate expressing empty vectors of Sm and Lg-BiTs. (B) Time course of the half-life of the Nano-Glo substrate after adding it a fixed concentration of the Lg-KRAS/Sm-CRAF. (C) Different construct arrangements of the Sm and the Lg with KRAS, p110 $\alpha$ , and RBD $\alpha$  tested by co-transfection into HEK293 cells. The addition of the Lg at the N-terminal of p110 $\alpha$  and RBD $\alpha$ , and the Sm to KRAS gives a strong and reliable signal of interaction. The negative control lysate comes from the transfection of HEK293 cells with empty Sm and Lg vectors. (D) 2D titration of individually expressed Lg-RBD $\alpha$  and Sm-KRAS (from 0.07–9  $\mu$ g/ $\mu$ l each). The coloured boxes illustrate the reduction in luminescence signal from the lower cell lysate concentrations. (E, F) The detection of the Sm-KRAS and the Lg-RBD $\alpha$  protein interaction produced from either individually expressed (E) or co-expressed HEK293 cell lysate (F). E, Lg-RBD $\alpha$  lysate was used at 8  $\mu$ g/ $\mu$ l and the Sm-KRAS was titrated at different concentrations. It required 0.2  $\mu$ g/ $\mu$ l Sm-KRAS + 8  $\mu$ g/ $\mu$ l Lg-RBD $\alpha$  to obtain a luminescence signal of ~1000 versus, 1  $\mu$ g/ $\mu$ l from the co-expressed lysate (F). (G) Titration of HEK293 cell lysate individually expressing Lg-KRAS, with fixed concentration of cell lysate 300 ng/ $\mu$ l expressing either Sm-CRAF (red) or Lg-KRAS/RBD $\alpha$ -DM as a negative control. (H, I) Competition assay titrating purified CRAF-RBD (0–400  $\mu$ M) individually expressed (D) or co-expressed (E) cell lysate of Sm-KRAS/Lg-RBD $\alpha$ . D, individually expressed lysate using Sm-KRAS at 5  $\mu$ g/ $\mu$ l with Lg-RBD $\alpha$ /DM at (2.3  $\mu$ g/ $\mu$ l), gave an IC<sub>50</sub> of about 300 nM. E, co-expressed Sm-KRAS/Lg-RBD $\alpha$  1  $\mu$ g/ $\mu$ l concentration, that gave an IC<sub>50</sub> of about 35nM. Calculated IC<sub>50</sub> values were determined using Prism 8.

The Lg-BiT enhances the solubility of poorly soluble proteins

We next employed the same methodology, co-transfection of HEK293 cells with the two constructs using the same BiBiT construct orientation, to detect the interaction of Lg-KRAS with either Sm-p110 $\alpha$  or Sm-p110 $\alpha$ -RBD (hereafter RBD $\alpha$ ) in the cell lysates. Since the interaction between KRAS and p110 $\alpha$  is substantially weaker than the RAS/RAF interaction, we titrated the cell lysate from 0.01–5  $\mu$ g/ $\mu$ l<sup>14</sup>. In the initial test, we failed to detect a significant signal of interaction between Lg-KRAS and Sm-p110 $\alpha$  or Sm-RBD $\alpha$  (Figure 3C)<sup>19</sup> and surmised that this was due to the poor solubility of the p110 $\alpha$  and RBD $\alpha$ <sup>21</sup>.

Since the Lg-BiT is the larger part of the NanoLuc protein and is properly folded, we hypothesized that switching the NanoBiT tags and adding the Lg-BiT on the N-terminal of p110 $\alpha$  and the RBD $\alpha$ , could improve the solubility of the proteins. We found that when co-transfecting Sm-KRAS with either Lg-p110 $\alpha$  or Lg-RBD $\alpha$ , we now detected a clear increase in signal of interaction between Sm-KRAS/Lg-p110 $\alpha$  and Sm-KRAS/Lg-RBD $\alpha$ , with an ideal lysate concentration range of 0.025–1.6  $\mu$ g/ $\mu$ l (Figure 3C)<sup>19</sup>. This suggests that fusion to the Lg-BiT can indeed improve the solubility of poorly soluble proteins. Since the signal obtained from the Sm-KRAS/Lg-RBD $\alpha$  was significantly stronger than the one obtained with the Sm-KRAS/Lg-p110 $\alpha$



interaction, we decided to continue our study using the isolated RBD $\alpha$  rather than full-length p110 $\alpha$ . In addition, we constructed an RBD $\alpha$  negative control (termed Lg-RBD $\alpha$ -DM) by inserting two mutations in the RBD $\alpha$  (T208D and K227A) that are known to block the interaction of p110 $\alpha$  with RAS<sup>12</sup>.

### Co-expression of Sm-KRAS/Lg-RBD $\alpha$ is more efficient than individual expression in detecting the complex interaction

We additionally tested the signal from Sm-KRAS/Lg-RBD $\alpha$  complex formation and the efficiency of the luminescence by expressing both proteins separately in HEK293 cells. We applied a two-dimensional (2D) titration of both Sm-KRAS and Lg-RBD $\alpha$  in 96 well plates to determine the concentration of each protein needed to give an ideal signal of PPI that could be used for drug screening. We found that using the Sm-RAS lysate at 4.5  $\mu\text{g}/\mu\text{l}$  with Lg-RBD $\alpha$  lysate at 9  $\mu\text{g}/\mu\text{l}$  gave a luminescence signal around 588 RLU (Relative Luminescence Signal) – intermediate between the highest (905 RLU) and the lowest (56 RLU) signal, which could be suitable for drug screening (Figure 3D)<sup>19</sup>. However, it appeared that greater quantities of cell lysates were needed from individually expressed Sm-RAS and Lg-RBD $\alpha$  than with the co-expressed lysate to obtain a comparable signal. This was further tested by titrating both co-expressed and individually expressed Sm-KRAS and Lg-RBD $\alpha$ /DM (Lg-RBD $\alpha$  or Lg-RBD $\alpha$ -DM). We observed that in the individually expressed lysates we needed around 0.2  $\mu\text{g}/\mu\text{l}$  Sm-KRAS + 8  $\mu\text{g}/\mu\text{l}$  Lg-RBD $\alpha$  to obtain an RLU signal of  $\sim$ 1000, whereas in the co-expressed lysate we only required 1  $\mu\text{g}/\mu\text{l}$  to reach a comparable level. The Lg-RBD-DM showed no signal increase with the individually expressed lysate, and only a slight signal increase (compared with the Sm-KRAS and Lg-RBD $\alpha$  signal) at higher concentrations in the co-expressed lysate (Figure 3E, F)<sup>19</sup>. However, in the case of Lg-KRAS and Sm-RAF, we did not witness a significant difference between co-expressed and individually expressed lysates when Lg-KRAS was titrated in the presence of 0.3  $\mu\text{g}/\mu\text{l}$  Sm-RAF (Figure 3G)<sup>19</sup>. The differences in signal strength between the individually and the co-expressed Sm-KRAS/Lg-RBD $\alpha$  experiments could be explained by the fact that in the co-expressed format the PPI happens prior to cell lysis and produces a relatively stable protein complex.

### The NBBA is responsive to the inhibition of protein interactions

Since the RAS/RAF interaction is about 150-fold stronger than RAS/p110 $\alpha$ , we used the RAF-RBD as a competitive inhibitor of the Sm-KRAS/Lg-RBD $\alpha$  interaction in the NBBA. We chose cell lysate concentrations that produce a signal of around 3–4-fold higher than the negative control to avoid high concentrations that may overwhelm the sensitivity of the assay in detecting PPI inhibition. We were also interested to compare the RAF-RBD inhibitory effect on Sm-KRAS/p110 $\alpha$  complex produced from either individually or co-expressed lysates. Firstly, with individually expressed protein lysates, Sm-KRAS was used at a concentration of 5  $\mu\text{g}/\mu\text{l}$  with 2.3  $\mu\text{g}/\mu\text{l}$  Lg-RBD $\alpha$ /DM. Second, co-transfected Sm-KRAS/Lg-RBD $\alpha$ -DM cell lysates were used at 0.5–1  $\mu\text{g}/\mu\text{l}$ . We then titrated

purified RAF-RBD from 400  $\mu\text{M}$ –0.015 nM. In both experimental formats, we observed a constant decline of the signal with the increase of the CRAF-RBD (Figure 3H, I)<sup>19</sup>. However, the individually expressed lysate format produced an estimated half-maximal inhibitory concentration (IC<sub>50</sub>) of 350 nM versus the co-expressed lysate IC<sub>50</sub> 35 nM which is closer to the generally accepted RAS/RAF complex affinity. This supports the notion that the co-expressed Sm-KRAS/Lg-RBD $\alpha$  cell lysate is the preferable format for the study of these PPIs.

### The NBBA is suitable for testing different types of inhibitors

We chose to investigate this system further by studying the efficiency of the NBBA response to other types of inhibitors. We selected three examples of recently described RAS inhibitors: Pan-RAS inhibitor 1344 (hereafter 1344), which is a weak binder of RAS ( $K_d \sim 17 \mu\text{M}$ ), a stronger KRAS inhibitor BI-2852 ( $K_d \sim 750 \text{ nM}$ ), and mutation-specific covalent KRAS-G12C inhibitor, ARS-1620<sup>22–24</sup>. In the case of 1344, we tested again the two types of cell lysate, co-expressed KRAS/Lg-RBD $\alpha$ /DM and individually expressed KRAS together with Lg-RBD $\alpha$  or Lg-RBD $\alpha$ -DM. The cell lysates were then treated with several concentrations of the 1344 inhibitor (2, 10, 50 and 250  $\mu\text{M}$ ) for 20 min prior to the addition of the Nano-Glo reagent. We found that 1344 was able to inhibit the Sm-KRAS/Lg-RBD $\alpha$  PPI in a dose dependent manner and did so more efficiently in the co-expressed lysate – similar to our earlier observations with RAF-RBD inhibition (Figure 4A, B)<sup>19</sup>.

Based upon the above observations, we decided to continue our studies using only the co-expressed lysate. We tested the effect of the KRAS inhibitor BI-2852 on the co-expressed Sm-KRAS/Lg-RBD $\alpha$  starting with lower inhibitor concentrations (0.1, 1, 10 and 100  $\mu\text{M}$ ) since it is a stronger inhibitor than 1344. The BI-2852 was also able to inhibit the Sm-KRAS/Lg-RBD $\alpha$  PPI in a dose dependent manner starting from around 1  $\mu\text{M}$  concentration (Figure 4C)<sup>19</sup>.

Furthermore, we also tested the covalent RAS-G12C inhibitor ARS-1620 on the co-expressed Sm-KRAS/Lg-RBD $\alpha$  and Lg-KRAS/Sm-RAF PPI. The ARS-1620 predominantly targets the RAS-GDP state, therefore it is important to test its effects in live cells where the impact on GDP/GTP exchange can be assessed. Both Sm-KRAS/Lg-RBD $\alpha$  and Lg-KRAS/Sm-RAF were co-transfected in HEK293 cells for 48 hr. The cells were then treated with either 2 or 10  $\mu\text{M}$  ARS-1620 for a further 4 hr. Cells were then harvested, lysed, sonicated and the cell lysis was quantified for PPI detection. We found that the ARS-1620 was indeed capable of reducing the signal of KRAS/Lg-RBD $\alpha$  and Lg-KRAS/Sm-RAF PPI at 2  $\mu\text{M}$  and at 10  $\mu\text{M}$  concentration (Figure 4D, E)<sup>19</sup>. These results demonstrate that the NBBA is also suitable for studying the effects of covalent inhibitors on PPIs.

### The NBBA can detect other PI3K family RBD interactions with RAS and has an excellent Z' value

It was previously published that RAS proteins only interact with certain isoforms of PI3K, namely p110 $\alpha$ ,  $\gamma$  and  $\delta$ , but not with p110 $\beta$ <sup>14</sup>. We therefore decided to test whether

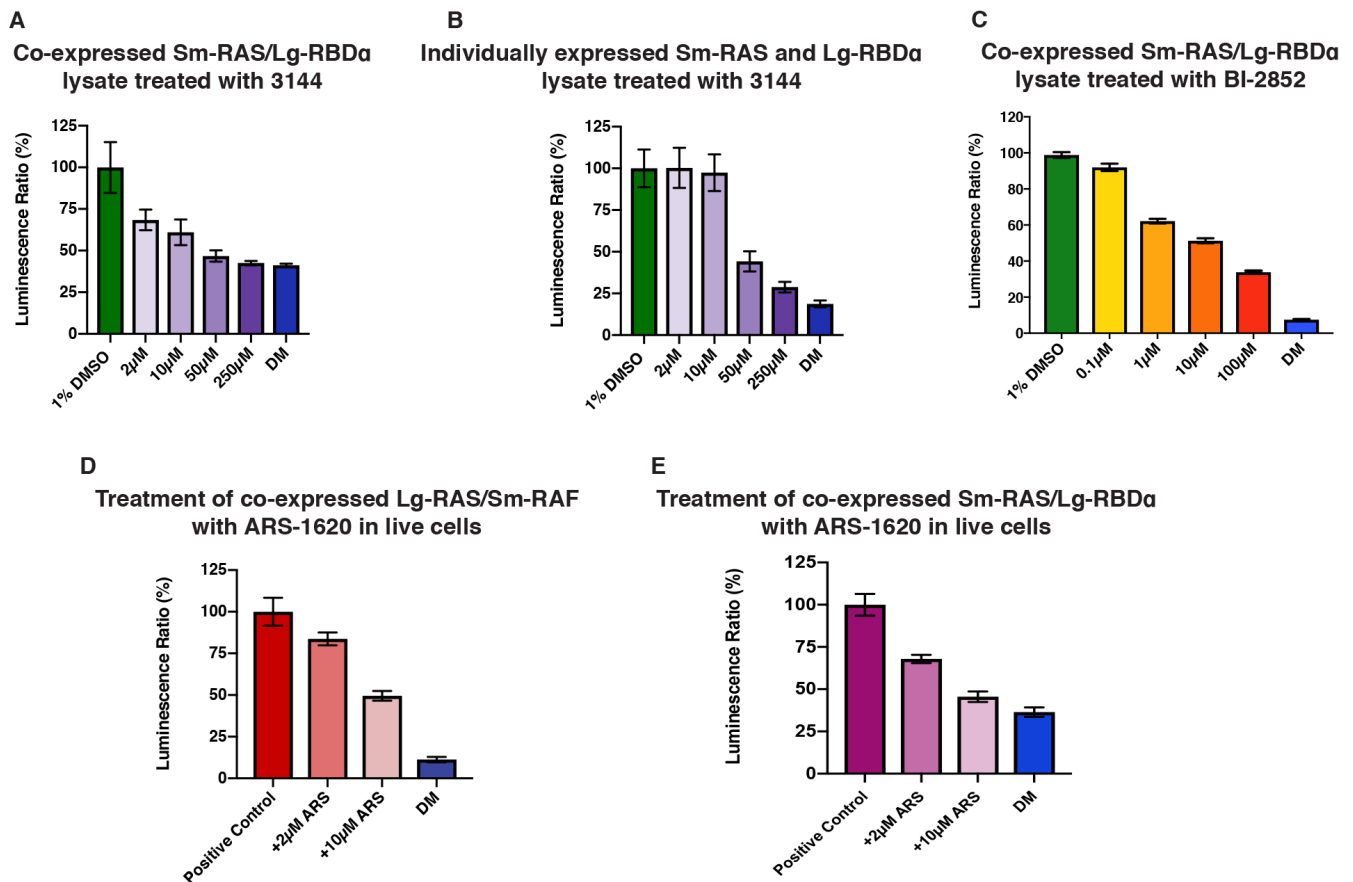


**Figure 4.** The NanoBit biochemical assay (NBBA) is responsive to different inhibitors. (A, B) The treatment of co-expressed Sm-RAS/Lg-RBDα (1 μg/μl) (A), or individually expressed Sm-RAS and Lg-RBDα at (0.5 μg/μl KRAS and 2.3 μg/μl Lg-RBDα) (B), with several concentrations of the PAN RAS inhibitor 1344 (2, 10, 50 and 200 μM). The positive control was treated with 1% DMSO equivalent to the concentration of DMSO in the highest 1344 concentration (200 μM). (C) Treatment of co-expressed Sm-RAS/Lg-RBDα using with the BI-2852 KRAS inhibitor at (0.1, 1, 10, and a 100μM) concentrations. (D, E) Treatment of HEK293 cells expressing either, Lg-KRAS/Sm-RAF (D) or Sm-KRAS/Lg-RBDα (E) with two concentrations the KRAS-G12C specific covalent inhibitor ARS-1620 (2 and 10 μM).

the NBBA is capable of distinguishing the different interacting isoforms of PI3K with RAS. The RBDs of p110γ, δ, and β were expressed as fusions with the Lg-BiT and tested in co-transfection with Sm-KRAS. The cell lysates of Sm-KRAS with either Lg-RBDγ, δ or β, were titrated at various concentrations by serial dilution, Nano-Glo was added and the effects analysed. The results clearly showed that Sm-KRAS interacts with p110γ and δ, but not with p110β (Figure 5A–C)<sup>19</sup>.

In order to test if the NBBA would be suitable and sufficiently reproducible for measuring PPI in a drug screening setting, it was important to determine the Z' factor value across different wells in a 384-well plate and across several different plates<sup>25</sup>. The co-expressed Sm-KRAS/Lg-RBDα/DM lysate was aliquoted across multiple 384 well plates at 10 μl and 20 μl reaction volume – followed by the addition of Nano-Glo (2 and 4 μl, respectively). Both reaction volumes, 10 μl and 20 μl, showed excellent Z' values of 0.5 and 0.7, respectively across the 384 wells, and Z' value of above 0.5 across different plates, demonstrating that the NBBA is a robust and

reliable assay for high throughput PPI and drug screening (Figure 5D–G)<sup>19</sup>.

#### Establishing stable cell lines expressing the Lg-RAS/Sm-RAF for high-throughput screening

We wanted to test the feasibility of generating cell lines that stably express the target proteins instead of employing transient expression. This would enable the production of cell lysate expressing the target proteins in a more robust and cost-effective manner. Thus, we generated CHO (Chinese hamster ovary) stable cell lines expressing the Lg-KRAS/Sm-CRAF protein complex (using the same vectors that were used in the transient transfection). The cells were seeded on plates (10 cm) and harvested after 24 hr, cell lysate was then quantified and titrated in 384-well plates as a 10 μl reaction volume (Figure 6A)<sup>19</sup>. We then applied our established experimental procedure to the cell lysate and observed that we can indeed obtain a signal of Lg-KRAS and Sm-CRAF similar to the transient expression signal (Figure 6B)<sup>19</sup>. In addition, as a negative control, we used a Sm-CRAF-R89L (hereafter Sm-RAS-M) construct



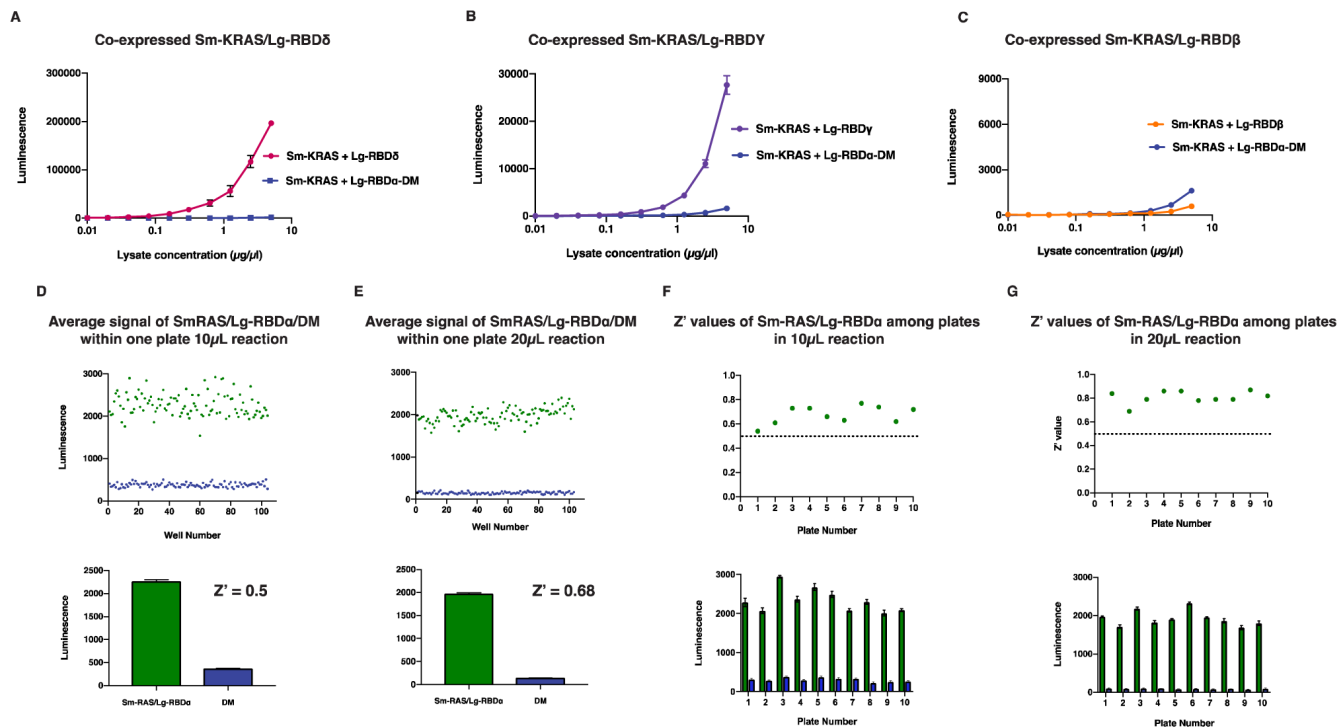


**Figure 5. The NanoBit biochemical assay (NBBA) can detect other PI3K family RBD interactions with RAS and has an excellent  $Z'$  value.** (A–C) Titration co-expressed Sm-KRAS with Lg-RBD $\delta$  (A), RBD $\gamma$  (B) and RBD $\beta$  (C). Both Lg-RBD $\delta$  and  $\gamma$  showed interaction with Sm-KRAS whereas Lg-RBD  $\beta$  did not. (D, E) Co-expressed Sm-KRAS/Lg-RBD $\alpha$  titrated (at 1  $\mu\text{g}/\mu\text{l}$ ) in different wells ( $n=104$ ) across a 384 well plate in 10  $\mu\text{l}$  (D) and 20  $\mu\text{l}$  (E) reaction volumes – along with the negative control Sm-KRAS/Lg-RBD $\alpha$ -DM. Top, scatter plots of luminescence signal arising from each well. Bottom, average of all 104 wells from the 10- $\mu\text{l}$  ( $Z' = 0.5$ ) and 20- $\mu\text{l}$  ( $Z' = 0.68$ ) reaction volume. (F, G) Co-expressed Sm-KRAS/Lg-RBD $\alpha$  titrated (at 1  $\mu\text{g}/\mu\text{l}$ ) across 10 wells ( $n=6$ ) across 10 plates in a 10  $\mu\text{l}$  (F) and 20  $\mu\text{l}$  (G) volume – along with the negative control Sm-KRAS/Lg-RBD $\alpha$ -DM. Top, scatter plots of the average  $Z'$  value from each plate. Bottom, average luminescence signal from each plate.

that carries a single amino acid point mutation and is known to block interaction with<sup>26</sup>. The lysate was responsive to ARS-1620 inhibitor (Figure 6C)<sup>19</sup>. Furthermore, we used an automated dispenser to titrate the cell lysate in eight different 384 plates to calculate the  $Z'$  value. We found that all eight plates gave excellent  $Z'$  values above 0.58 (Figure 6D)<sup>19</sup>, further supporting the notion that the NBBA assay is suitable for automated high throughput screening.

## Discussion

From these results, we conclude that the NBBA represents a useful development of the NanoBit live cell assay. The NBBA is simple and easy to use: for example, the cell lysates of the proteins of interest can be expressed, either by transient transfection or from stable cell lines, in high quantities, quantified and stored in aliquots at  $-80^{\circ}\text{C}$  for multiple usages. Moreover, since the reaction volumes are only 10 or 20  $\mu\text{l}$ , only small quantities of Nano-Glo reagent are needed, which makes it a cost-effective assay. The NBBA is a sensitive assay for detecting both strong and weak PPI. In addition, the Lg-BiT provides an extra function along with its essential luminescence role, as it

can improve the solubility of poorly soluble proteins – such as the RBDs of PI3K. Furthermore, we showed that the NBBA is suitable for detecting PPI inhibition using four examples of inhibitors: a strong protein competitor protein RAF-RBD, a weak small molecule pan RAS inhibitor 1344, a stronger KRAS inhibitor BI-2852, and a covalent small molecule KRAS G12C inhibitor ARS-1620. In addition, the NBBA is suitable for use at small scale by transient expression in cells or at high scale using stable cell line expression of the target proteins of interest. Finally, the NBBA produces excellent  $Z'$  values, which makes it a suitable assay for PPI or drug screening.

Interaction of RAS proteins with their effector enzymes underpins key aspects of both normal cellular growth control and also the aberrant proliferation seen in the roughly 15% of cancers that express mutationally activated RAS oncogenes. Many approaches have been taken to attempting to inhibit RAS oncoprotein function, but it has proven to be an extremely challenging drug target<sup>6</sup>. One possible angle is to screen for small molecule inhibitors of the interaction of RAS with its effectors, either RAF or PI3K isoforms. Screening the RAS/

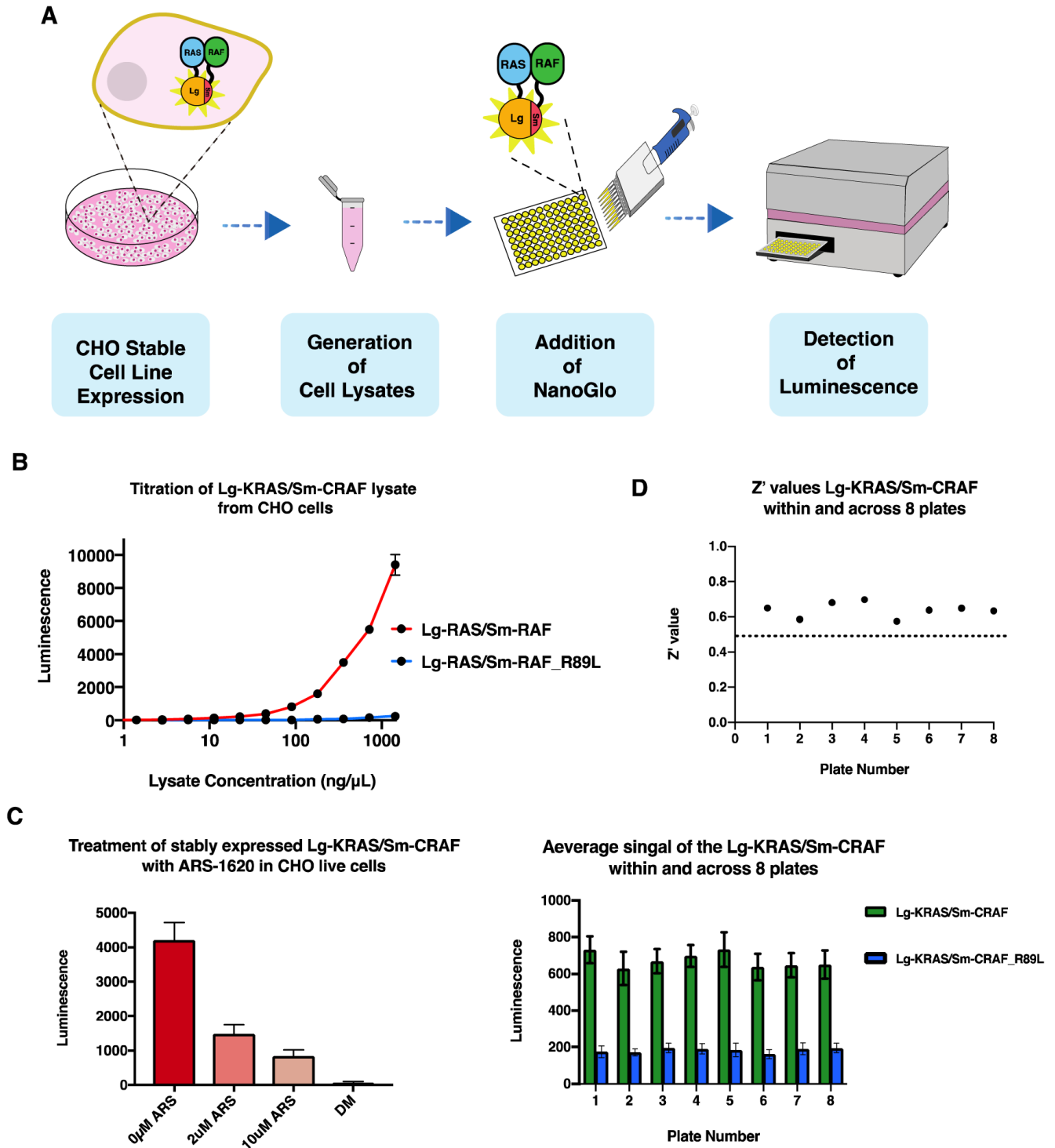


**Figure 6.** The NanoBit biochemical assay (NBBA) functions in stable cell line expression. **(A)** Schematic diagram representing the steps required for the protein expression in stable cell lines. CHO stably expressing Sm-KRAS/Lg-CRAF cells are seeded on plates, cells are then harvested after 24hrs, titrated into 384 well plates followed by the addition of the Nano-Glo for detecting the protein interaction. **(B)** Titration of CHO cell lysate stably expressing Sm-KRAS/Lg-CRAF. The signal of interaction is similar to the ones obtained from transient expression. **(C)** Treatment of the Sm-KRAS/Lg-CRAF cell lysate arriving from CHO cells with ARS-1620. There is a clear inhibition of the KRAS/CRAF interaction at 2 μM and 10μM ARS-1620. **(D)** Measuring the Z' value, the Sm-KRAS/Lg-CRAF cell lysate in 8x 384 well plates using an automated dispenser. Top, scatter plot representing the Z' value of each plate. Bottom, average luminescence signal from all 385 wells in each plate (green bars). Blue bars show the negative control (Sm-KRAS/Lg-CRAF-R89L).

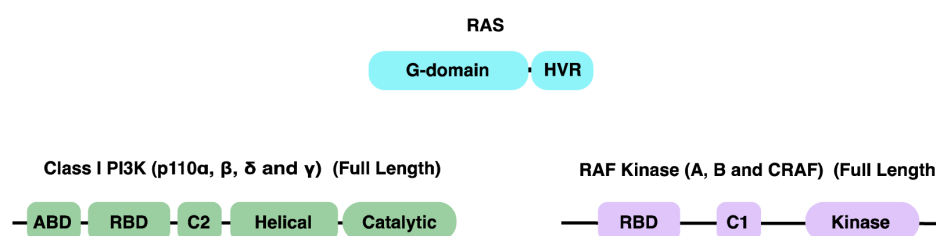
RAF interaction has long been feasible, for example using HTRF assays or alpha screens. However, possibly due to the tight nature of this interaction, it has not proven possible to find inhibitors from screening libraries in this way. As the interaction of RAS with PI3K is some 150-fold weaker, we surmise that it may be far easier to detect compounds in screens that will interfere with this weak interaction. We can speculate as to why the NBBA overcomes previous difficulties in developing reliable high throughput assays for this interaction of RAS with PI3K: one possibility is that the interaction between these two proteins is stabilized to some extent by the very weak (~200  $\mu$ M) interaction of the fusion split luciferase partners<sup>14</sup>. In addition, the correct post-translational modification of the proteins achieved in this human cell line derived expression





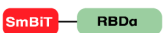







system might also prove advantageous. In any case, the NBBA for the interaction of RAS with PI3K may provide an ideal setting for identifying inhibitors of this interaction in high throughput screens. More broadly, this biochemical, cell-free derivative of the NanoBiT split-luciferase cell-based assay may be very useful for high throughput screening for inhibitors of a number of important protein-protein interactions.

## Methods

### Construct generation and cloning

All constructs with their abbreviations are listed in [Figure 7](#). All inserts of the constructs used in this study are derived from human cDNA. The following full-length cDNA KRAS-G12C and p110 $\alpha$ , and the PI3K-RBDs (RBD $\alpha$  aa133-314,



Construct Abbreviation	Construct Full Name
Sm-KRAS 	SmBiT-KRAS-G12C (Full Length)
Sm-RAF 	SmBiT-CRAF (Full Length)
Sm-RAF-M 	SmBiT-CRAF-M (Full Length) R89L mutant
Sm-p110 $\alpha$ 	SmBiT-p110 $\alpha$ (Full Length)
Sm-RBD $\alpha$ 	SmBiT-RBD $\alpha$ (aa133-314)
Lg-KRAS 	LgBiT-KRAS-G12C (Full Length)
Lg-p110 $\alpha$ 	LgBiT-p110 $\alpha$ (Full Length)
Lg-RBD $\alpha$ 	LgBiT-p110 $\alpha$ (aa133-314)
Lg-RBD $\alpha$ -DM 	LgBiT-p110 $\alpha$ -DM (aa133-314) (T208D and K227A) Double Mutant
Lg-RBD $\beta$ 	LgBiT-p110 $\beta$ (aa141-288)
Lg-RBD $\delta$ 	LgBiT-p110 $\delta$ (aa134-288)
Lg-RBD $\gamma$ 	LgBiT-p110 $\gamma$ (aa170-309)

**Figure 7. Abbreviations of SmBiT- and LgBiT- tagged protein constructs used in the NanoBiT assay.** A diagram (top) to represent the domain structures of the current proteins used in the NanoBiT assay. The table illustrates the shorthand name and the full-length name of the SmBiT and LgBiT constructs used, with illustrations that correspond to the domain structure diagrams above.

RBD $\beta$  aa141-288, RBD $\delta$  aa134-288 and RBD $\gamma$  aa170-309 were cloned using BiBiT NanoBiT vectors: pBiT2.3-N [CMV/SmBiT/Blast] Vector (pRSG199) or pBiT1.3-N [CMV/LgBiT/Hyg] Vector (pRSG197), using InFusion<sup>®</sup> Cloning and primer design (Takara Bio) using SacI and BamHI restriction sites. A list of the primer sequences used in this study is in Table 2. Both full-length Lg-KRAS-G12C and Sm-RAF were provided by Promega ready cloned into pBiT1.1-N [TK/LgBiT] and pBiT2.1-N [TK/SmBiT], respectively. Both Lg-KRAS-G12C and Sm-RAF were also sub-cloned in BiBiT NanoBiT vectors. The p110 $\alpha$  regulatory subunit (p85 $\alpha$ ) was sub-cloned into pcDNA3 vector.

PCR amplification of full length or target fragments of cDNA were carried out using the reagents and conditions listed in Table 3. Following agarose gel electrophoresis of PCR products, DNA was extracted and purified with the QIAquick PCR Purification Kit according to the manufacturer's instructions. Inserts and vectors were added in an approximate molar ratio of 1 (vector): 8 (insert) and left at room temperature for 1 hour, followed by transformation. All new vector/insert mix were transformed into *E. coli* DH5- $\alpha$  competent cells: 20 min incubation on ice, 45 s heat shock at 42°C, followed by 3 min incubation on ice, then grown in SOC (Super Optimal Broth) medium for 1 hour prior to distribution onto Kanamycin LB agar

plates prior to growth overnight (o/n). Colonies were picked and inoculated in LB broth o/n with kanamycin (60  $\mu$ g/ml). Mini-preps and Sanger sequencing of plasmids were carried out by the Genomics Equipment Park at the Francis Crick Institute. Mini-preps were re-transformed and inoculated in 250 ml LB broth overnight and maxipreps were carried out using the QIAGEN<sup>®</sup> Plasmid Maxi Kit according to the manufacturer's instructions. Maxiprep plasmids were used for the transfection in HEK293 cells. For mutant constructs, site-directed mutagenesis (SDM) of previously cloned SmBiT (RAF) and LgBiT (p110 RBD $\alpha$ ) constructs was performed with PCR and plasmids were digested with 1  $\mu$ l DpnI restriction enzyme (10 U/ $\mu$ l) (NEB) at 37°C for 1 hour – followed by transformation in DH5- $\alpha$  as above.

#### Transfection and lysis of HEK293 cells

HEK293 cells were acquired as growing cultures from the Francis Crick Cell Services Platform and maintained (at 37°C and 5% CO<sub>2</sub>) in DMEM (Dulbecco's Modified Eagle Medium) (Gibco<sup>™</sup>, 41966-029) supplemented with fetal bovine serum (FBS) (v/v 10%) (SIGMA F7524), L-Glutamine (3 mM) (SIGMA G7513), and Penicillin-Streptomycin antibiotics (100 units/ml) (SIGMA P4333). Prior to transfection, cells were seeded into 10-cm or 15-cm dishes for 24 hours. Co-transfection and individual transfection of SmBiT and LgBiT constructs

**Table 2. List of primer sequences that have been used in this study.**

Forward KRAS Full length – LgBiT/SmBiT SacI	CGAGCGGTGGAGCTCAGATGACTGAATATAAACTTGTGG
Reverse KRAS Full length – LgBiT/SmBiT BamHI	AGAACCGCCGGATCCCTACATAATTACACACTTTGTCTTTGAC
Forward p110 $\alpha$ full length LgBiT/SmBiT SacI	CGAGCGGTGGAGCTCAGATGCCTCCAAGACCATCATCAGG
Reverse p110 $\alpha$ full length LgBiT/SmBiT BamHI	AGAACCGCCGGATCCCTAGTTCAATGCATGCTGTTAATTGTG
Forward RBD $\alpha$ 133-314 LgBiT/SmBiT SacI	CGAGCGGTGGAGCTCAGGATCCAGAAGTACAGGACTTCCG
Reverse RBD $\alpha$ 133-314 LgBiT/SmBiT BamHI	AGAACCGCCGGATCCCTAAGCTGTGGAATGCGTCTGG
Forward RBD $\beta$ 134-288 LgBiT SacI	CGAGCGGTGGAGCTCAGAAGGATCCTGAAGTAAATGAATTCG
Reverse RBD $\beta$ 134-288 LgBiT BamHI	AGAACCGCCGGATCCCTACTTGCAGCATTCCACAAGTATAAAATGG
Forward RBD $\delta$ 134-288 LgBiT SacI	CGAGCGGTGGAGCTCAGTTGTGCGACCCAGAAGTGAACG
Reverse RBD $\delta$ 134-288 LgBiT BamHI	AGAACCGCCGGATCCCTACCTCGCCATGCGGGATGAG
Forward RBD $\lambda$ 170-309 LgBiT SacI	CGAGCGGTGGAGCTCAGGACGATGAGCTGGAGTTCACG
Reverse RBD $\lambda$ 170-309 LgBiT BamHI	AGAACCGCCGGATCCCTACGTGTCCAGTACCACGTGAATC
Forward p110 $\alpha$ T208D LgBiT	AATGACAAGCAGAAGTATGATCTGAAAATCAACCATGAC
Reverse p110 $\alpha$ T208D LgBiT	GTCATGGTTGATTTTCAGATCATACTTCTGCTTGTCAAT
Forward p110 $\alpha$ K227A LgBiT	AAGCAATCAGGGCAAAAACCTCGAAG
Reverse p110 $\alpha$ K227A LgBiT	CAACATACTCGAGTTTTTGCCTGATTGCTTCAGCAAT
Forward CRAF K89L LgBiT	AAAGCACTCAAGGTGTTGGGCTGCAACCAGAG
Reverse CRAF K89L LgBiT	CTCTGGTTGCAGGCCCAACACCTTGAGTGCTTT

**Table 3. PCR reagents and conditions. (A)** Table of reagents (KOD polymerase, Novagen, C133158, primers Sigma Life Science) and volumes used for the PCR amplification of inserts and vectors which were used to clone new SmBiT and LgBiT constructs. All reactions were carried out at a total volume of 50  $\mu$ l. **(B)** The conditions used for PCR amplification for cloning and SDM.

**A.**

Reagent	Volume $\mu$ L
KOD Hot Start Polymerase Buffer 10X	1
MgSO <sub>4</sub> 25mM	3
dNTPs 2mM	5
KOD Hot Start DNA Polymerase	1
Forward Primer 10 $\mu$ M	1.5
Reverse Primer 10 $\mu$ M	1.5
Deionised H <sub>2</sub> O	37
DNA template (20-25ng)	X
Total	50

**B.**

Step	Temperature $^{\circ}$ C	Time	Cycle X
Denaturation	95	3 (min)	25X
Denaturation	95	30 (sec)	
Annealing	60	30 (sec)	
Extension	72	3 (min)	
Extension	72	10 (min)	
Incubation	12		

were carried out according to the manufacturer's instructions using FuGene HD Transfection Reagent (Promega, E2311) diluted with Opti-MEM<sup>TM</sup> (Gibco<sup>TM</sup>, 51985-026) at a ratio of 3 (FuGene.): 1  $\mu$ g (DNA). For individual transfection, 2  $\mu$ g and 7  $\mu$ g DNA were used in 10-cm and 15-cm dishes, respectively. In co-transfection experiments, 4  $\mu$ g and 14  $\mu$ g DNA in total were used for 10-cm and 15-cm dishes, respectively. In the case of Sm-KRAS and Lg-p110 $\alpha$  co-transfection, we also transfected an equal amount of p85 $\alpha$ -pcDNA, to ensure the stability and function of p110 $\alpha$  protein.

After 48 hr of transfection, media was removed and the cells were washed once with ice cold phosphate-buffered saline (PBS) buffer. The cells were then harvested in 1X Passive buffer (Promega), sonicated for 10 s and centrifuged at 4 $^{\circ}$ C for 10 min. The cell lysate was then quantified using a Protein Assay Kit (Bio-RAD, 500-0114), aliquoted (30  $\mu$ l in PCR tubes), snap frozen in liquid nitrogen and then stored at -80 $^{\circ}$ C.

### NBBA protocol for PPI detection

Cell lysates after quantification were titrated by 2-fold serial dilution using titration buffer (TB; 25 mM Tris pH8, 100 mM NaCl, 0.5 mM TCEP) in Corning<sup>TM</sup> 384-well plates (Greiner 784904). The concentration of the titration range was based on the affinity of interaction between the target proteins (Lg-KRAS/Sm-RAF 0.002–5  $\mu$ g/ $\mu$ l in 20  $\mu$ l and Sm-KRAS/Lg-PI3K proteins, from 0.01–10  $\mu$ g/ $\mu$ l). The Nano-Glo Live Cell Substrate (Promega, N2012) was diluted in (Nano-Glo Live Cell Substrate (LCS) buffer, Promega, N2068) 1:20 to obtain 1X concentration, and added as 4  $\mu$ l/20  $\mu$ l reaction or 2  $\mu$ l/10  $\mu$ l reaction. Plates were then centrifuged 1000 rpm for 10–15 seconds and the luminescence signal was recorded immediately at time zero and every 5 min for 45 min, using PheraStar FSX Detection System (BMG Labtech). Negative controls, either Sm-RAS/Lg-RBD $\alpha$ -DM or Lg-RAS/Sm-RAF-M, at the same cell lysate concentration as the target PPI of interest were run in all experiments. These negative controls produced an average signal from 200–300 RLU. A signal of positive PPI was considered if it was above 3–4-fold higher than the signal arising from the negative.

Typical cell lysate serial dilutions for NBBA were produced as follows:

For a 10 $\mu$ l reaction example: for a titration range 0.002–5  $\mu$ g/ $\mu$ l (12 titrations), 8  $\mu$ l of TB was added to all tubes (with the exception of the first tube). The cell lysate was diluted to 5  $\mu$ g/ $\mu$ l in 16- $\mu$ l volume. Next, 8  $\mu$ l was taken from the first tube and mixed with the 2<sup>nd</sup> tube, then 8  $\mu$ l was taken from the 2<sup>nd</sup> tube and mixed with the 3<sup>rd</sup> tube. This process was repeated to the last titration concentration 0.002  $\mu$ g/ $\mu$ l (tube 12). This was followed by the addition of 2 $\mu$ l 1X Nano-Glo to all 12 tubes.

For a 20  $\mu$ l reaction example: similar to above, with the exception that first the cell lysate was diluted at 5  $\mu$ g/ $\mu$ l in 32- $\mu$ l volume. Then, 16  $\mu$ l from the first tube was used for mixing with the rest of the tubes (already containing 16  $\mu$ l TB). This was followed by the addition of 4  $\mu$ l of 1X Nano-Glo. A schematic presentation of the titration steps is illustrated in (Figure 8).

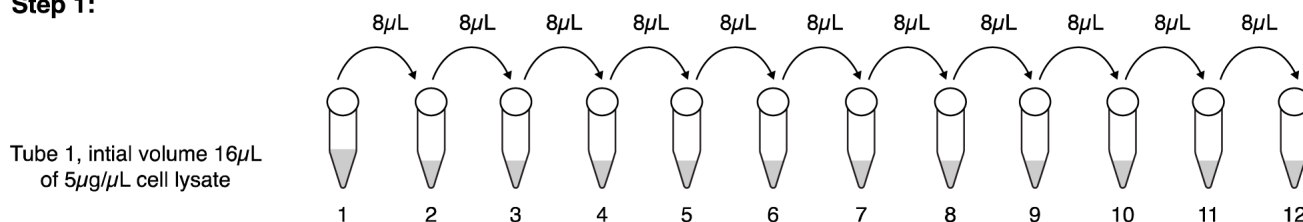
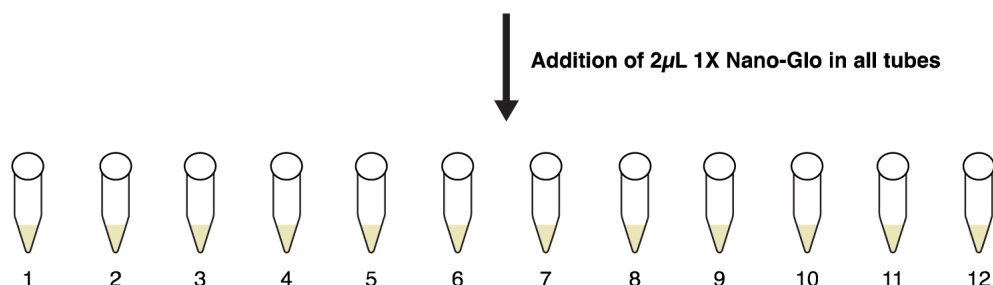
Note 1: as protein expression will vary to some extent in each transfection, we ensured with every new lysate that we applied the above titration steps to determine the optimum lysate concentration needed to detect a reliable interaction signal (3–4 fold higher than the negative control). As described above, the cell lysate was then aliquoted, snap frozen in liquid nitrogen and stored in the -80 $^{\circ}$ C.

Note 2: When cell lysate aliquots were thawed after storage at -80 $^{\circ}$ C, we also repeated the above titration steps to ensure that the PPI was unaffected by freezing and had not lost activity.

### NBBA protocol for PPI inhibition

In all the PPI inhibition experiments we adopted the following procedure:



**Step 1:****Step 2:**

**Figure 8. Schematic representation of a 10 µl NBBA reaction preparation.** Step 1: An example of a cell lysate titration experiment ranging from 0.002–5 µg/µl concentration (12 tubes). The cell lysate will be diluted in TB at a concentration of 5 µg/µl in 16 µl volume. The rest of the tubes will contain 8 µl TB. The titration steps start by taking 8 µl from the 1<sup>st</sup> tube and mixing it in the 2<sup>nd</sup> tube, this step is repeated until tube 12. Step 2: The addition of 2 µl Nano-Glo reagent in all tubes. The above steps present the NBBA reaction preparation in tubes, however the same procedures are also applied in 384 well plates. For the 20 µl NBBA reaction, the same steps are the same with the exception that the first tube will contain 5 µg/µl cell lysate in 32 µl volume, followed by the addition of 4 µl 1X Nano-Glo.

The cell lysate concentration of a positive PPI was selected at the point where it gave a luminescence signal 3–4-fold higher than the negative control (i.e. positive PPI signal 1000–1200 RLU and the negative control 200–300 RLU). This was to ensure that the lysate concentration was sufficiently high to detect the PPI, but not too high to detect a weak PPI inhibitor.

After incubation of the inhibitors with the cell lysate (producing the PPI of interest), and the addition of Nano-Glo, plates were centrifuged (as above) and the signal was collected immediately for 45 min.

#### Competition assay

Co-expressed Sm-KRAS/Lg-RBDα 1 µg/µl, and the individually expressed Sm-KRAS, 0.5 µg/µl and Lg-RBDα 5 µg/µl were aliquoted in 19 wells. Lg-RBDα-DM served as a negative control. Purified RAF-RBD was titrated in all wells in a serial 2-fold dilution from 4–0.000015 µM. The plate was incubated on ice for 15 min, followed by the addition of 4 µl 1X Nano-Glo (per 20-µl reaction volume), and the luminescence signal was measured.

#### 1344 Pan RAS inhibitor experiment

The co-expressed Sm-KRAS/Lg-RBDα/DM at 0.5 µg/µl, and the individually expressed Sm-KRAS with Lg-RBDα or Lg-RBDα-DM (0.5 µg/µl KRAS and 2.3 µg/µl Lg-RBDα/DM), were aliquoted in multiple wells, and the 1344 was added at (2, 10, 50 and 250 µM) and incubated on ice for 20 min. Following addition of 4 µl 1X Nano-Glo (per 20-µl reaction volume), the luminescence signal was measured. The highest concentration of the 1344 inhibitor (250 µM) contained a

1%DMSO in the final concentration of NBBA reaction, therefore we used a control reaction of 1%DMSO alone as a vehicle.

#### ARS-1620 experiment

HEK293 cells were seeded in 10-cm plates, and co-transfected with Sm-RAS and Lg-RBDα/DM (as described above). After 48 hr of transfection, the cells were treated with 2 and 10 µM ARS-1620 for 4 hr. The cells were then harvested and lysed in Passive buffer, sonicated and the cell lysates were quantified. The ARS-1620 cell lysates were aliquoted in multiple wells along with the control (untreated) Sm-KRAS/Lg-RBDα cell lysate). Following addition of 4 µl 1X Nano-Glo (per 20 µl reaction volume), the luminescence signal was measured.

#### Stable cell line development and maintenance

Lg-KRAS and Sm-CRAF were selected for the generation of stable cell lines. Constructs were transfected and selected separately. ExpiCHO-S cells were diluted to a density of  $2 \times 10^6$  cells/mL in 10 mL of Gibco ExpiCHO Expression Medium (Thermo Fisher Scientific). For transfection, 2 µg of DNA was diluted in reduced serum medium Opti-Pro (Thermo Fisher Scientific) to a total volume of 0.6 mL. Transfection reagents ExpiFectamine CHO (Thermo Fisher Scientific) were diluted at a ratio of 1:2.7 (plasmid: reagent) in reduced serum medium in a total volume of 0.6 mL. The solution was incubated at room temperature for 1 minute. After incubation, diluted DNA and transfection reagents were mixed and incubated for 5 minutes. The mixture was added to the cells drop by drop. Cells were incubated at 37°C in a 125-rpm shaker incubator with 8% CO<sub>2</sub> for 24 hours and then diluted to  $1 \times 10^6$  cells/mL in 30 mL medium with 250 µg/mL of Geneticin

(Thermo Fisher Scientific). Every 3–4 days, cells were selected and diluted in medium with Geneticin until they reached the usual ExpiCHO-S cell division rate of 3 times every 24 hours. Once the division rate became stable and cell viability was maintained at >98%, transfection of the second DNA constructs was carried out using the same procedure as the first transfection. Transfected cells were selected by both 250 µg/mL of Geneticin and 200 µg/mL of Hygromycin B (Biovision).

### Protein expression and purification

KRAS-G12C expression, purification and loading with GppNHP (Sigma G0635-5MG) or GDP (Sigma G7252) was performed using established protocols<sup>14</sup>.

p110 $\alpha$ : details outlining construction of plasmids used to express the p110 $\alpha$  and p85 $\alpha$  subunits of PI3K are given previously<sup>14</sup>. Sf21 (Life Technologies) insect cells were co-infected with baculoviruses encoding GST-fusions of the p110 $\alpha$  and p85 $\alpha$  subunits and cultures allowed to grow at 27°C with shaking for three days. Cell pellets were then harvested and stored at -80°C until required. For purification, the thawed cell pellets were resuspended in buffer containing 50 mM HEPES (pH 8.0), 250 mM NaCl, 10% glycerol, 10 mM  $\beta$ -glycerophosphate, 1 mM EDTA, 1 mM NaF, 10 mM benzamidine, 1 mM DTT and protease inhibitor cocktail (Roche), lysed by sonication and centrifuged to remove insoluble material. PI3K complexes were extracted from the soluble fraction of the lysate by affinity chromatography using glutathione agarose (GE Healthcare). Complexes were then cleaved from the resin by overnight digestion with HRV 3C protease, purified by gel-filtration and snap frozen in buffer containing 50 mM HEPES (pH8.0), 200 mM NaCl, 5% glycerol, 1 mM DTT.

### HTRF assays

KRAS-G12C/CRAF-RBD interaction: biotinylated RAS-G12C\_GppNHP or GDP were labelled with the donor dye Streptavidin-Europium, and GST-CRAF-RBD was labelled with anti-GST XL665 dye as an acceptor. Anti-GST XL665-CRAF-RBD was mixed at 10nM with 5nM of either Streptavidin-Europium-RAS-G12C\_GppNHP or GDP, incubated for 15min and data collected using the plate reader (PheraStar FSX Detection System (BMG Labtech)).

KRAS-G12C/p110 $\alpha$  interaction: for the first experiment, 10 nM of Anti-GST-p110 $\alpha$  labelled with XL665 (acceptor) were mixed with 3µM Streptavidin-Europium-RAS-G12C\_GppNHP or GDP (donor). For the second experiment, 10nM of Europium-GST-p110 $\alpha$  (donor) was mixed with Streptavidin-XL665-RAS-G12C\_GppNHP or GDP (acceptor). In both experiments the reactions were incubated for 15min and data collected as above.

### Data analysis

All experiments were performed in replicates of n=3, including the blank control wells (Nano-Glo in titration buffer). At the selected time points, measurements of all reactions were averaged and subtracted from the average signal of the blank control value. The average signals were plotted and fitted to lines and

curves using GraphPad Prism 8. Z-prime (Z') values, the statistical parameter used to assess the quality of a screening assay, were calculated using the formula:

$$Z' = 1 - \frac{3\sigma_+ + 3\sigma_-}{|\mu_+ + \mu_-|}$$

where  $\sigma_-$  and  $\sigma_+$  represent the standard deviation of the luminescence signal of the positive control (Sm-KRAS and Lg-RBD $\alpha$ ) and negative control (Sm-KRAS and Lg-RBD $\alpha$ -DM) respectively and  $\mu_-$  and  $\mu_+$  represent the mean luminescence signal of the positive control and negative control respectively.  $0 < Z' < 0.5$  represents a 'do-able assay' and  $0.5 \leq Z' < 1$  represents an 'excellent assay'<sup>25</sup>.

### Data availability

#### Underlying data

Open Science Framework: NBBA (NanoBit Biochemical Assay). <https://doi.org/10.17605/OSF.IO/MGKQV><sup>19</sup>.

This project contains the following underlying data:

- **All plates analysis (CSV):**

All the plates were analysed to obtain the mean and the SEM (Standard error mean) and plot the data for each experiment/figure.

- **Figure 2–Figure 6 (CSV):**

Figure 2 A–C: HTRF assay of KRAS with RAF and p110 $\alpha$

Figure 2 A–C: HTRF assay of KRAS with RAF and p110 $\alpha$ , analysis

Figure 3A: Titration of Lg-KRAS/Sm-RAF

Figure 3A: Titration of Lg-KRAS/Sm-RAF, analysis

Figure 3B: Nano-Glo Time course

Figure 3C: LgRAS\_Sm-p110 $\alpha$  expression

Figure 3C: Sm-KRAS/Lg-p110 $\alpha$  and Lg-RBD $\alpha$

Figure 3C: LgRAS\_Smp110 $\alpha$  expression, analysis

Figure 3D: 2D titration of Sm-KRAS/Lg-RBD $\alpha$

Figure 3D: 2D titration of Sm-KRAS/Lg-RBD $\alpha$ , analysis

Figure 3E: Individual expression Sm-KRAS/Lg-RBD $\alpha$

Figure 3E: Individual expression Sm-KRAS/Lg-RBD $\alpha$ , analysis

Figure 3F: Co-expression of Sm-KRAS/Lg-RBD $\alpha$

Figure 3F: Co-expression of Sm-KRAS/Lg-RBD $\alpha$ , analysis

Figure 3G: Individually expression of Lg-KRAS/Sm-RAF

Figure 3G: Individually expression of Lg-KRAS/Sm-RAF, analysis

Figure 3H: Individually expressed Sm-KRAS/Lg-RBD $\alpha$  Competition experiment

Figure 3I: Co-expressed Sm-KRAS/Lg-RBD $\alpha$  Competition experiment

Figure 4A-B: PAN RAS inhibitor 1344

Figure 4A-B: PAN RAS inhibitor 1344, analysis

Figure 4C: KRAS inhibitor BI-2852 experiment

Figure 4C: KRAS inhibitor BI-2852 experiment, analysis

Figure 4D: ARS-1620 inhibitor with Lg-RAS/Sm-RAF

Figure 4D: ARS-1620 inhibitor with Lg-RAS/Sm-RAF, analysis

Figure 4E: ARS-1620 inhibitor with Sm-RAS/Lg-p110 $\alpha$

Figure 4E: ARS-1620 inhibitor with Sm-RAS/Lg-p110 $\alpha$ , analysis

Figure 5A–C: Co-expression of Sm-KRAS/Lg-RBD $\alpha$  delta, gamma and beta

Figure 5A–C: Co-expression of Sm-KRAS/Lg-RBD $\alpha$  delta, gamma and beta, analysis

Figure 5D: Z' of Sm-KRAS/Lg-RBD $\alpha$  10 $\mu$ L reaction across 1 plate

Figure 5D: Z' of Sm-KRAS/Lg-RBD $\alpha$  10 $\mu$ L reaction across 1 plate, analysis

Figure 5E: Z' of Sm-KRAS/Lg-RBD $\alpha$  20 $\mu$ L reaction across 1 plate

Figure 5E: Z' of Sm-KRAS/Lg-RBD $\alpha$  20 $\mu$ L reaction across 1 plate, analysis

Figure 5F–G:

Z' of Sm-KRAS/Lg-RBD $\alpha$  10 and 20 $\mu$ L reaction across 10 plates, Plate 1

Z' of Sm-KRAS/Lg-RBD $\alpha$  10 and 20 $\mu$ L reaction across 10 plates, Plate 2

Z' of Sm-KRAS/Lg-RBD $\alpha$  10 and 20 $\mu$ L reaction across 10 plates, Plate 3

Z' of Sm-KRAS/Lg-RBD $\alpha$  10 and 20 $\mu$ L reaction across 10 plates, Plate 4

Z' of Sm-KRAS/Lg-RBD $\alpha$  10 and 20 $\mu$ L reaction across 10 plates, Plate 5

Z' of Sm-KRAS/Lg-RBD $\alpha$  10 and 20 $\mu$ L reaction across 10 plates, Plate 6

Z' of Sm-KRAS/Lg-RBD $\alpha$  10 and 20 $\mu$ L reaction across 10 plates, Plate 7

Z' of Sm-KRAS/Lg-RBD $\alpha$  10 and 20 $\mu$ L reaction across 10 plates, Plate 8

Z' of Sm-KRAS/Lg-RBD $\alpha$  10 and 20 $\mu$ L reaction across 10 plates, Plate 9

Z' of Sm-KRAS/Lg-RBD $\alpha$  10 and 20 $\mu$ L reaction across 10 plates, Plate 10

Z' of Sm-KRAS/Lg-RBD $\alpha$  10 and 20 $\mu$ L reaction across 10 plates, analysis

Figure 6B: CHO expression of Lg-KRAS/Sm-RAF

Figure 6B: CHO expression of Lg-KRAS/Sm-RAF, analysis

Figure 6C: ARS-1620 treatment on CHO expression of Lg-RAS/Sm-RAF

Figure 6C: ARS-1620 treatment on CHO expression of Lg-RAS/Sm-RAF, analysis

Figure 6D:

Z' of CHO expressed Lg-KRAS/Sm-RAF 10 $\mu$ L reaction, Plate 1

Z' of CHO expressed Lg-KRAS/Sm-RAF 10 $\mu$ L reaction, Plate 2

Z' of CHO expressed Lg-KRAS/Sm-RAF 10 $\mu$ L reaction, Plate 3

Z' of CHO expressed Lg-KRAS/Sm-RAF 10 $\mu$ L reaction, Plate 4

Z' of CHO expressed Lg-KRAS/Sm-RAF 10 $\mu$ L reaction, Plate 5

Z' of CHO expressed Lg-KRAS/Sm-RAF 10 $\mu$ L reaction, Plate 6

Z' of CHO expressed Lg-KRAS/Sm-RAF 10 $\mu$ L reaction, Plate 7

Z' of CHO expressed Lg-KRAS/Sm-RAF 10 $\mu$ L reaction, Plate 8

Z' of CHO expressed Lg-KRAS/Sm-RAF 10 $\mu$ L reaction, analysis

- **Figure 2–Figure 6 analysis (all CSV):**

In all figures, we presented the normalised or the relative luminescence/Fluorescence data of each experiment.

Data are available under the terms of the [Creative Commons Attribution 4.0 International license](#) (CC-BY 4.0).

---

#### Author contributions

M.I. and J.D. designed the study, interpreted the results and wrote the manuscript. M.I., R.C., N.K., N.S.H., J.T., C.R., R.G. and D.C.H. performed the biochemical experiments. J.T., B.F.B. and K.V.W. provided expertise and reagents. All authors contributed to manuscript revision and review.

#### Acknowledgements

We thank Miriam Molina for helpful discussion and critical reading of the manuscript and the science technology platforms at the Francis Crick Institute including Bioinformatics and Biostatistics, Genomics Equipment Park, Structural Biology and Cell Services.

## References

1. Degorce F, Card A, Soh S, *et al.*: **HTRF: A technology tailored for drug discovery - a review of theoretical aspects and recent applications.** *Curr Chem Genomics.* 2009; **3**: 22–32.  
[PubMed Abstract](#) | [Publisher Full Text](#) | [Free Full Text](#)
2. Janzen WP: **Screening technologies for small molecule discovery: the state of the art.** *Chem Biol.* 2014; **21**(9): 1162–1170.  
[PubMed Abstract](#) | [Publisher Full Text](#)
3. Hancock JF: **Ras proteins: different signals from different locations.** *Nat Rev Mol Cell Biol.* 2003; **4**(5): 373–384.  
[PubMed Abstract](#) | [Publisher Full Text](#)
4. Killoran RC, Smith MJ: **Conformational resolution of nucleotide cycling and effector interactions for multiple small GTPases determined in parallel.** *J Biol Chem.* 2019; **294**(25): 9937–9948.  
[PubMed Abstract](#) | [Publisher Full Text](#) | [Free Full Text](#)
5. Knickelbein K, Zhang L: **Mutant KRAS as a critical determinant of the therapeutic response of colorectal cancer.** *Genes Dis.* 2015; **2**(1): 4–12.  
[PubMed Abstract](#) | [Publisher Full Text](#) | [Free Full Text](#)
6. McCormick F: **Progress in targeting RAS with small molecule drugs.** *Biochem J.* 2019; **476**(2): 365–374.  
[PubMed Abstract](#) | [Publisher Full Text](#)
7. Stephen AG, Esposito D, Bagni RK, *et al.*: **Dragging ras back in the ring.** *Cancer Cell.* 2014; **25**(3): 272–281.  
[PubMed Abstract](#) | [Publisher Full Text](#)
8. Li S, Balmain A, Counter CM: **A model for RAS mutation patterns in cancers: finding the sweet spot.** *Nat Rev Cancer.* 2018; **18**(12): 767–777.  
[PubMed Abstract](#) | [Publisher Full Text](#)
9. Simanshu DK, Nissley DV, McCormick F: **RAS Proteins and Their Regulators in Human Disease.** *Cell.* 2017; **170**(1): 17–33.  
[PubMed Abstract](#) | [Publisher Full Text](#) | [Free Full Text](#)
10. Bivona TG: **Dampening oncogenic RAS signaling.** *Science.* 2019; **363**(6433): 1280–1281.  
[PubMed Abstract](#) | [Publisher Full Text](#)
11. Castellano E, Sheridan C, Thin MZ, *et al.*: **Requirement for interaction of PI3-kinase p110 $\alpha$  with RAS in lung tumor maintenance.** *Cancer Cell.* 2013; **24**(5): 617–630.  
[PubMed Abstract](#) | [Publisher Full Text](#) | [Free Full Text](#)
12. Gupta S, Ramjaun AR, Haiko P, *et al.*: **Binding of ras to phosphoinositide 3-kinase p110 $\alpha$  is required for ras-driven tumorigenesis in mice.** *Cell.* 2007; **129**(5): 957–968.  
[PubMed Abstract](#) | [Publisher Full Text](#)
13. Fischer A, Hekman M, Kuhlmann J, *et al.*: **B- and C-RAF display essential differences in their binding to Ras: the isotype-specific N terminus of B-RAF facilitates Ras binding.** *J Biol Chem.* 2007; **282**(36): 26503–26516.  
[PubMed Abstract](#) | [Publisher Full Text](#)
14. Fritsch R, de Krijger I, Fritsch K, *et al.*: **RAS and RHO families of GTPases directly regulate distinct phosphoinositide 3-kinase isoforms.** *Cell.* 2013; **153**(5): 1050–1063.  
[PubMed Abstract](#) | [Publisher Full Text](#) | [Free Full Text](#)
15. Pacold ME, Suire S, Perisic O, *et al.*: **Crystal structure and functional analysis of Ras binding to its effector phosphoinositide 3-kinase gamma.** *Cell.* 2000; **103**(6): 931–943.  
[PubMed Abstract](#) | [Publisher Full Text](#)
16. Dixon AS, Schwinn MK, Hall MP, *et al.*: **NanoLuc Complementation Reporter Optimized for Accurate Measurement of Protein Interactions in Cells.** *ACS Chem Biol.* 2016; **11**(2): 400–408.  
[PubMed Abstract](#) | [Publisher Full Text](#)
17. Johnston PA, Johnston PA: **Cellular platforms for HTS: three case studies.** *Drug Discov Today.* 2002; **7**(6): 353–363.  
[PubMed Abstract](#) | [Publisher Full Text](#)
18. Wang Z, Wang X, He Z, *et al.*: **[Establishment of drug screening assay and pharmacodynamic evaluation method targeting influenza RNA polymerase].** *Yao Xue Xue Bao.* 2012; **47**(9): 1159–1163.  
[PubMed Abstract](#)
19. Ismail M: **NBBA (NanoBit Biochemical Assay).** 2020.  
<http://www.doi.org/10.17605/OSF.IO/MGKQV>
20. Winter JJ, Anderson M, Blades K, *et al.*: **Small molecule binding sites on the Ras:SOS complex can be exploited for inhibition of Ras activation.** *J Med Chem.* 2015; **58**(5): 2265–2274.  
[PubMed Abstract](#) | [Publisher Full Text](#)
21. Athuluri-Divakar SK, Vasquez-Del Carpio R, Dutta K, *et al.*: **A Small Molecule RAS-Mimetic Disrupts RAS Association with Effector Proteins to Block Signaling.** *Cell.* 2016; **165**(3): 643–655.  
[PubMed Abstract](#) | [Publisher Full Text](#) | [Free Full Text](#)
22. Janes MR, Zhang J, Li LS, *et al.*: **Targeting KRAS Mutant Cancers with a Covalent G12C-Specific Inhibitor.** *Cell.* 2018; **172**(3): 578–589 e517.  
[PubMed Abstract](#) | [Publisher Full Text](#)
23. Welsch ME, Kaplan A, Chambers JM, *et al.*: **Multivalent Small-Molecule Pan-RAS Inhibitors.** *Cell.* 2017; **168**(5): 878–889 e829.  
[PubMed Abstract](#) | [Publisher Full Text](#) | [Free Full Text](#)
24. Kessler D, Gmachl M, Mantoulidis A, *et al.*: **Drugging an undruggable pocket on KRAS.** *Proc Natl Acad Sci U S A.* 2019; **116**(32): 15823–15829.  
[PubMed Abstract](#) | [Publisher Full Text](#) | [Free Full Text](#)
25. Zhang JH, Chung TD, Oldenburg KR: **A Simple Statistical Parameter for Use in Evaluation and Validation of High Throughput Screening Assays.** *J Biomol Screen.* 1999; **4**(2): 67–73.  
[PubMed Abstract](#) | [Publisher Full Text](#)
26. Fabian JR, Vojtek AB, Cooper JA, *et al.*: **A single amino acid change in Raf-1 inhibits Ras binding and alters Raf-1 function.** *Proc Natl Acad Sci U S A.* 1994; **91**(13): 5982–5986.  
[PubMed Abstract](#) | [Publisher Full Text](#) | [Free Full Text](#)

# Open Peer Review

Current Peer Review Status: ? ?

## Version 1

Reviewer Report 22 April 2020

<https://doi.org/10.21956/wellcomeopenres.17179.r38408>

© 2020 Bery N. This is an open access peer review report distributed under the terms of the [Creative Commons Attribution License](#), which permits unrestricted use, distribution, and reproduction in any medium, provided the original work is properly cited.

? **Nicolas Bery** 

Cancer Research Centre of Toulouse, INSERM, Université Toulouse III Paul Sabatier, CNRS, Toulouse, France

Cooley *et al.* have implemented a biochemical assay from a cell-based split luciferase assay to monitor RAS protein-protein interaction (PPI) and RAS PPI inhibition. They show the development and use of this cell free assay as method to detect RAS PPI inhibition by small molecule inhibitors (three published RAS inhibitors) and one macromolecule (CRAF RBD). This study is well described, with the appropriate controls and the data presented supports their conclusions. The main advantage of this method is its potential application to high throughput screening (HTS) of small molecule inhibitors of PPI and this approach could be extended to any mutant RAS/effector interaction of choice. Overall, the methods provided in the manuscript give enough details to replicate the experiments but some information is missing. The authors should address these minor points:

1. Usually optimisation steps are needed for these kind of PPI probes (e.g. linker length and probes orientation). However, no information is provided concerning the optimisation procedures that were employed to get the KRAS/effectors NanoBiT probes with the exception of the orientation of the SmBiT/LgBiT molecules on CRAF full-length and KRAS<sup>G12C</sup>. Therefore, it is unclear whether the NanoBiT KRAS/effector probes described in this study can be further optimised. This is important information to know for potential future users:
  - It should be indicated whether the linker length between the Lg/SmBiT and KRAS/effectors was optimised. Their sequence should be added in the methods section.
  - All the RBDs (CRAF and PI3Ks) are tagged on their amino terminal end with a NanoBiT probe (Sm/LgBiT). It should be explained whether the opposite tagging combination (on the carboxy terminal end of the RBDs) was tested and compared to N terminal end tagging. For example, the structural data available for HRAS/CRAF RBD (PDB ID 4G3X, 4G0N) show that the N terminal end of HRAS is closer to the C terminal end of CRAF RBD, which suggests that cloning the Sm/LgBiT on the C terminal end of this RBD might give an optimal luciferase complementation and a higher luminescence signal.
2. The expression of the NanoBiT probes in the cell lysates should be controlled by Western blotting.



3. Additional information should be provided regarding the incubation time of the inhibitors in the cell lysates used in this study (20 minutes): how was this time chosen? Was it optimised?
4. In the methods section, the details of BI-2852 inhibitor treatment is not indicated (including the incubation time), the missing information should be added.
5. Figure 3: panels H/I: the authors should indicate in the figure legend what the dotted lines represent in these panels.

**Is the rationale for developing the new method (or application) clearly explained?**

Yes

**Is the description of the method technically sound?**

Yes

**Are sufficient details provided to allow replication of the method development and its use by others?**

Partly

**If any results are presented, are all the source data underlying the results available to ensure full reproducibility?**

Yes

**Are the conclusions about the method and its performance adequately supported by the findings presented in the article?**

Yes

**Competing Interests:** No competing interests were disclosed.

**Reviewer Expertise:** Development of cell-based assays to monitor PPI, targeting PPI with inhibitors (small molecules and macromolecules).

**I confirm that I have read this submission and believe that I have an appropriate level of expertise to confirm that it is of an acceptable scientific standard, however I have significant reservations, as outlined above.**

Author Response 14 May 2020

**Julian Downward**, Francis Crick Institute, London, UK

**Authors' Response to Reviewer Report from Nicolas Bery**

**Point 1:**

With regard to the linker length and sequence, in the case of N terminal, Lg-KRAS-G12C and Sm-RAF in pBiT1.1-N [TK/LgBiT] and pBiT2.1-N [TK/SmBiT] vectors respectively, these vectors were provided by Promega for our initial studies to test the assay. Both vectors (either N terminal Sm or Lg-BiT) contained the same exact linker sequence encoding 13 amino acids (GGGGSGGGSAIA). They were not further optimised. However, in the case of the BiBiT vectors pBiT2.3-N [CMV/SmBiT/Blast] Vector (pRSG199) or pBiT1.3-N [CMV/LgBiT/Hyg] Vector

(pRSG197) that we used for the rest of our studies, the restriction sites SacI and BamHI were introduced to provide an N terminal linker of 18 amino acids (GSSGGGGSGGGGSSGGAQ), 5 amino acids longer than that in the other vectors. Nevertheless, we did see a good signal arising from the RAS-G12C and the p110-RBDs, so we did not apply any further optimisation to the linker length or sequence. The linker sequences have been added in the paper.

As regards the orientation of the tags, the initial vectors provided by Promega expressing N terminal Lg-KRAS and N terminal Sm-CRAF produced a strong signal, indicating that placing the tags at the N termini of both proteins did not block or prevent the production of a strong luminescence signal that indicates the RAS/CRAF interaction. Therefore, we employed the same orientation of the tags on the BiBiT vectors for Sm-KRAS G12C and p110-RBDs. Further, in the case of the p110-RBDs, due to the fact that they are not very soluble, we also considered placing the Lg-BiT on the N terminus to ensure that it can provide maximum solubility to the RBDs. We managed to produce a significant signal representing the interaction of RAS and the p110-RBDs. Therefore, we did not try different orientations for the tag in the case of the p110-RBDs. In the case of RAS, we considered it to be important to have the tag on the N terminus and not the C terminus to avoid any prevention of RAS localisation to the cellular membrane. Although this was our rationale for the tag orientations for our study with these target proteins, we would recommend that other studies with different protein targets should test all tag orientation combinations.

**Point 2:**

Due to the lack of an efficient antibody for the Lg-BiT we used antibodies against KRAS, CRAF and p110 $\alpha$  to detect the transiently expressed proteins. We added a new figure in the paper (Figure 7) where we show an increase in the signal intensity and/or increased molecular weight (due to the addition of the Sm or the Lg-BiT tags) between the transiently expressed and the endogenous proteins.

**Point 3:**

The 20 minute incubation was chosen to ensure full target engagement of inhibitors with RAS. As one of the inhibitors used in the study (Pan RAS 3144) is a weak binder, we wanted to give the maximum opportunity for the inhibitor to bind to RAS. We tested both 20 and 30min but saw no difference by increasing the time to 30min. Therefore we added the 20min time-point. However we recommend for other inhibitors and protein targets that shorter or longer incubation times should be tested. This has been added in the materials and methods section.

**Point 4:**

The BI-2852 information has been added to the methods section. The same treatment and experimental condition was used as for the Pan RAS 3144 inhibitor.

**Point 5:**

The figure legend of Figure 3H, I has been corrected to describe the dotted lines.

**Competing Interests:** None

Reviewer Report 17 February 2020

<https://doi.org/10.21956/wellcomeopenres.17179.r37848>

© 2020 Stephen A. This is an open access peer review report distributed under the terms of the [Creative Commons Attribution License](#), which permits unrestricted use, distribution, and reproduction in any medium, provided the original work is properly cited. The author(s) is/are employees of the US Government and therefore domestic copyright protection in USA does not apply to this work. The work may be protected under the copyright laws of other jurisdictions when used in those jurisdictions.



**Andrew G. Stephen**

NCI RAS Initiative, Cancer Research Technology Program, Frederick National Laboratory for Cancer Research, Frederick, MD, USA

Cooley and co-authors have adapted a cell based split luciferase assay originally designed for intracellular protein:protein interactions into a biochemical assay using cellular lysates. The authors apply this approach to measuring the interaction between KRAS and PI3Ka, which has previously been characterized as a relatively weak interaction. One significant benefit of this approach could be the improved solubility of the proteins in the HEK292 cells, which the authors claim combination of the largeBiT fragment with PI3K appears to improve solubility (although they do not show any direct evidence of this). Optimal signals were obtained between KRAS and PI3Ka-RBD rather than full length PI3Ka. The assay is specific as PI3K mutants do not bind and CRAF-RBD effectively competes. Cooley *et al.* also show the interaction between PI3K-RBD and KRAS is inhibited by 3 previously characterized RAS inhibitors and provide data that supports the assay is amenable to small molecule screening in 384 well plates. The methods are described in enough detail that would allow replication by others and the authors outline the benefits/limitations of working with cell lysates rather than live cells. Overall the manuscript provides a new approach for interrogating the interaction between PI3K and RAS and can be adapted as an HTS compatible assay for other binding partners with low solubility or weak binding affinity. The following minor issues should be addressed:

1. While Cooley *et al.* were unable to use HTRF to detect the binding of recombinant KRAS and PI3Ka, Kessler *et al.* (2019)<sup>1</sup> published a method using alpha technology to detect their interaction and showed inhibition by BI2852. A reference should be made to this work and a brief comment made of the differences between the HTRF approach reported here and the alpha assay described by Kessler *et al.*
2. The authors clearly show that no specific interaction was observed between KRAS and PI3Ka irrespective of which protein was the acceptor or the donor. However, when KRAS was labeled with streptavidin-europium the fluorescence signal was  $\sim 10^5$  times larger than the KRAS-CRAF-RBD experiment or when PI3Ka was labeled with europium (compare Figure 2B with 2A or 2C). The statement in the text indicating “only a low signal was achieved (Figure 2B, C)” is confusing and the authors should clarify.

## References

1. Kessler D, Gmachl M, Mantoulidis A, Martin LJ, et al.: Drugging an undruggable pocket on KRAS. *Proc Natl Acad Sci U S A*. 2019; **116** (32): 15823-15829 [PubMed Abstract](#) | [Publisher Full Text](#)

**Is the rationale for developing the new method (or application) clearly explained?**

Yes

**Is the description of the method technically sound?**

Yes

**Are sufficient details provided to allow replication of the method development and its use by others?**

Yes

**If any results are presented, are all the source data underlying the results available to ensure full reproducibility?**

Yes

**Are the conclusions about the method and its performance adequately supported by the findings presented in the article?**

Yes

**Competing Interests:** No competing interests were disclosed.

**Reviewer Expertise:** Biochemical and biophysical analysis of RAS and RAS effector interactions.

**I confirm that I have read this submission and believe that I have an appropriate level of expertise to confirm that it is of an acceptable scientific standard, however I have significant reservations, as outlined above.**

Author Response 02 Apr 2020

**Julian Downward**, Francis Crick Institute, London, UK

We thank Andrew Stephen for his constructive comments. In response to the specific points, we now reference the paper by Kessler et al. (2019) describing the use of alpha technology to detect the interaction of KRAS and PI3Ka and show its inhibition by BI2852. Compared to our HTRF assay, the alpha assay was run using lower KRAS concentrations (10nM versus 3µM), but similar PI3Ka levels (10nM). We have clarified the statement about the level of fluorescence signal in Figure 2B: the signal strength was high, but not GTP dependent, so considered to be non-specific.

**Competing Interests:** No competing interests were disclosed.

Author Response 14 May 2020

**Julian Downward**, Francis Crick Institute, London, UK

**Authors' Response to Reviewer Report by Andrew Stephens**

We thank Stephens for his comments. In response to the specific points, we now reference the paper by Kessler et al. (2019) describing the use of alpha technology to detect the interaction of KRAS and PI3Ka and show its inhibition by BI2852. Compared to our HTRF assay, the alpha assay was run using lower KRAS concentrations (10nM versus 3µM), but similar PI3Ka levels (10nM). We have clarified the statement about the level of fluorescence signal in Figure 2B: the signal strength was high, but not GTP dependent, so considered to be non-specific.

**Competing Interests:** None

